Investigation of Dynamic and Static Pile Behavior from Modified Standard Penetration Tests

by

Frank Rausche[1], Gabriel Thendean[1], Hasan Abou-matar[1], Garland Likins[1], and George Goble[1]

INTRODUCTION

The widespread utilization of Standard Penetration Test (SPT) for in-situ soil investigations both in the United States and in many other countries makes it economically and technically desirable to extract more quantitative information than merely an N-value from this test. The SPT has often been criticized for inaccuracies, primarily because of an uncertain energy reaching the sampler during its driving. Schmertmann and Palacios (1979) indicated that the energy delivered to the rod can vary from 30 to 80% of the theoretical one. The test, however, produces both a quantitative strength value and a soil sample. Furthermore, modern measurement techniques make a very realistic assessment of sampler driving energy a simple task, and therefore the uncertainty about the transferred energy can be eliminated. In addition, many applications require that the SPT N-values be adjusted to an average energy level before it is used, for example the assessment of liquefaction potential of sand (Seed et al., 1985).

Wave equation analyses of the pile driving process also have become very popular in recent years. This method allows for the computation of blow count and pile stresses based on hammer, driving system, pile and soil information. Wave equation analyses have as a goal (a) the replacement of the dynamic formula for bearing capacity predictions based on the blow count at the end of pile driving, and (b) the prediction of the pile driving progress (drivability) based on accurate soil information. While bearing capacity assessment is always an important issue when static load testing is difficult or impossible, drivability predictions are particularly important for large piles which require expensive installation equipment, *e.g.*, in the offshore or nearshore environment.

Traditional wave equation analyses, based on the concept of E. A. L. Smith (1960), were primarily lacking in the description of the soil behavior. The current model has two important parameters, the flexibility or quake of the soil-pile interface resistance and the damping factor which describes the increased dynamic resistance of the soil-pile interface relative to the static resistance. Since the SPT sampler experiences the same type of rapid acceleration as a driven pile it is not unreasonable to expect that careful measurements during sampler driving would allow for a more accurate prediction of the wave equation soil parameters than current practice which uses experience values based solely on the grain size distribution of the soil. The SPT procedure with additional measurements is referred to as the Modified SPT.

To successfully predict wave equation soil parameters from measurements taken during SPT sampler driving, it first must be ascertained that the dynamic soil resistance acting on the sampler can be described with reasonable accuracy by the soil model of Smith. Actually, the study described here also investigated more complex soil models as described in the literature

[1]Goble Rausche Likins and Associates, Inc., Cleveland, OH 44128, USA

(such as Coyle and Gibson, 1970; Erickson, 1990; Heerema and De Jong, 1979; Randolph, 1987, and Niyama, 1992), and indeed it appeared to be necessary to include at least two additional parameters in the SPT soil model, namely a hyperbolic end bearing behavior and a soil plug mass. However, for full scale piles, these two parameters were ignored and only Smith's damping and quake were assessed using SPT information.

This paper describes the Modified SPT procedure including measurements techniques, analysis methods and a summary of results. It also shows correlations of the wave equation analysis predictions with static load test results on full scale piles. The wave equation analyses were performed utilizing the soil parameters calculated from the Modified SPT results.

DESCRIPTION OF THE MODIFIED SPT

Owing to the many error sources in the bearing capacity and drivability calculations by wave equation analysis, the objectives of the Modified SPT measurements were rather varied. First, resistance on the sampler included both shaft resistance and end bearing effects. Thus, the tests had to be devised such that they allowed for a separation of shaft resistance and end bearing effects.

Second and most importantly, the damping factors were to be measured and/or calculated since they appeared to be the most important soil resistance parameter responsible for prediction errors (assuming that the hammer and driving system performance had been verified). Dynamic measurements during sampler driving yields a total dynamic resistance. However, since according to Smith (and that is also most widely accepted theory) the damping resistance is the difference between the total dynamic resistance and the static resistance, it is important for damping calculations that the static resistance is known. Thus both static and dynamic measurements had to be taken. Static measurements are somewhat susceptible to both loading rate effects and setup (increasing soil resistance with time). Both effects are also important for wave equation predictions. Therefore, static measurements had to be conducted at different loading rates and after different waiting times.

Finally, the static flexibility or quake had to be evaluated. Experience with dynamic pile measurements had shown that the toe quake often was much larger than commonly assumed and therefore caused poor predictions of pile stresses and bearing capacity values. With these requirements in mind, the procedure described in Table 1 was developed and the necessary equipment whose main components we described below were designed and built.

MEASUREMENT TECHNIQUES

Dynamic Force and Velocity Measurements

The Modified SPT procedure requires the measurement of dynamic force and velocity near the top of the SPT drill rod during sampler driving, and N-value counting. The force and velocity measurements are very similar to the routine measurements performed during dynamic testing of piles with the Pile Driving Analyzer® (PDA). The top force and velocity measurements were accomplished with foil gages and accelerometers, respectively, mounted at the midpoint of a

Table 1: The Modified SPT Procedure Items in *italics* were not to be performed in routine procedure	
1.	Advance drill hole to the required test depth and insert the split spoon sampler.
2.	Attached the instrumented rod to the top of the drill string just before mounting the hammer.
3.	Perform a normal SPT procedure (18 inches or 457 mm of sampler driving) while measuring force and velocity with the PDA, and the hammer impact velocity with the HPA.
4.	If N-value is less than 40: reduce the hammer drop height such that equivalent N-value is around 60 to 120, (i.e., rod penetration of 0.1 to 0.2 inch or 2.5 to 5.0 mm per blow).
5.	If the soil layer has a potential for setup: wait for 5 minutes and then restrike with at least two different hammer drop heights.
6.	If restrike in step 5 yields more than 20% set / blow: wait for 15 minutes, 1 hour, or possibly overnight and then restrike again with at least two different hammer drop heights.
7.	*Remove the hammer and perform static uplift tests at three different rates. Repeat the test after some wait period.*
8.	*Perform torque test after the static uplift test and before sampler extraction.*
9.	Extract sampler from drill hole, inspect, mark and save the sample.
10.	If N-value, extracted sample and uplift test suggest that the soil layer is significant for end bearing: Replace sampler with a special tip and re-insert the rod in the drill hole.
11.	Attach the instrumented rod, mount the hammer, and drive the tip at least six inches or 50 hammer blows whichever is achieved first; while taking the force velocity measurement.
12.	If the tip penetration is more than 0.2 inch (5 mm) per hammer blow: reduce the hammer drop height such that the above tip penetration is achieved.
13.	When relaxation is expected such that in a very dense silty sand, decompose shale, or shale, a 30-minute to 12-hour restrike should be performed.
14.	*Remove the hammer and performed a static compression test with at least three different loading rates. If relaxation is expected then repeat the static and dynamic test after some wait period.*
15.	Advance to the next sampling depth.

two foot long SPT drill rod section (Figure 1). Dynamic pile tests with the PDA have been routinely used in the United States and around the world, and have been very well documented for example Rausche (1994), Beim (1992), Fellenius et al. (1992), and Hussein and Rausche (1990).

Analog signals from strain gages and accelerometers were conditioned, digitized, and processed with a PDA, Model PAK, manufactured by Pile Dynamics Incorporated (PDI). Due to high frequency signals generated by the steel to steel impact between the hammer and anvil, a high sampling rate of 20 kHz was required when converting the signals to digital form. The PDA recorded the strain and acceleration signals from each hammer impact and converted them to force and velocity, respectively, before saving them to PDA's hard disk. The force and velocity records were also displayed on the PDA's liquid crystal display (LCD) screen for data quality evaluation.

In addition, a Hammer Performance Analyzer (HPA) was used to measure the SPT hammer impact velocities which were important for hammer kinetic energy calculations. The HPA, manufactured by PDI, uses the radar technology to measure the hammer velocities and plot them as a function of time on a strip chart. This device is also used for assessment of the pile driving hammer.

Oversized Tips

When the SPT N-value and the recovered sample suggested that the soil layer could have potential for significant end bearing or refusal pile driving, a special investigation of the soil's bearing capacity was performed. For this special test, the sampler was replaced by an oversized solid tip for better prediction of unit end bearing. The advantage of the oversized tip is a reasonable simulation of the pile end bearing condition without friction effects, since the tip is larger than the AW drill rod.

Two types of tip were investigated: the flat end and the cone tip, shown in Figure 2. The flat end tip was chosen since most displacement piles had flat bottom and therefore the flat end tip would simulate the real pile behavior. The cone tip was also investigated because of the widespread experience with cone penetration test (CPT) in soil investigation and since some closed end pipes were driven with conical point. Both types of oversized tip have an outside diameter of 2.5 inches (64 mm). This diameter gives the oversized tip an area of approximately 3 times the area of the standard CPT tip.

Axial Static Load Tests

Static load tests were performed at the end of sampler or oversized tip driving. The main purpose of performing the load tests was to determine directly the sampler shaft resistance or end bearing from the uplift and compression tests, respectively. To perform the load tests, a reaction frame was set around the drill hole behind the drill rig for both compressive and tensile reaction forces. The frame was set on and connected to a pair of hollow stem augers, one on each side of the drill hole, which were screwed into the ground. A center hole, 60-ton (533-kN) hydraulic jack provided uplift or compression loads by pushing against the top or bottom of the reaction beam. Figure 3 shows the schematic reaction frame setup for the uplift and compression tests. The top and middle figures show the hollow stem augers, reaction frame,

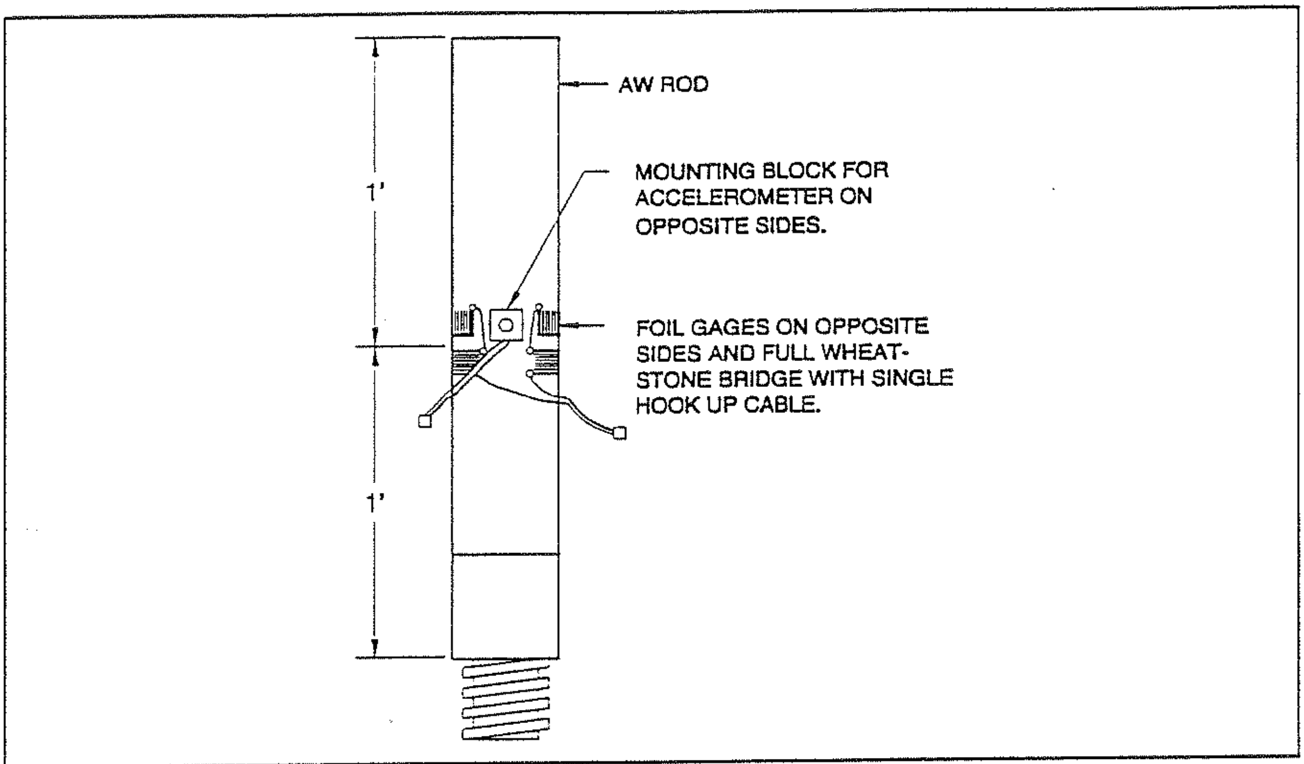

Figure 1: Instrumented SPT Rod (1' = 0.305 m)

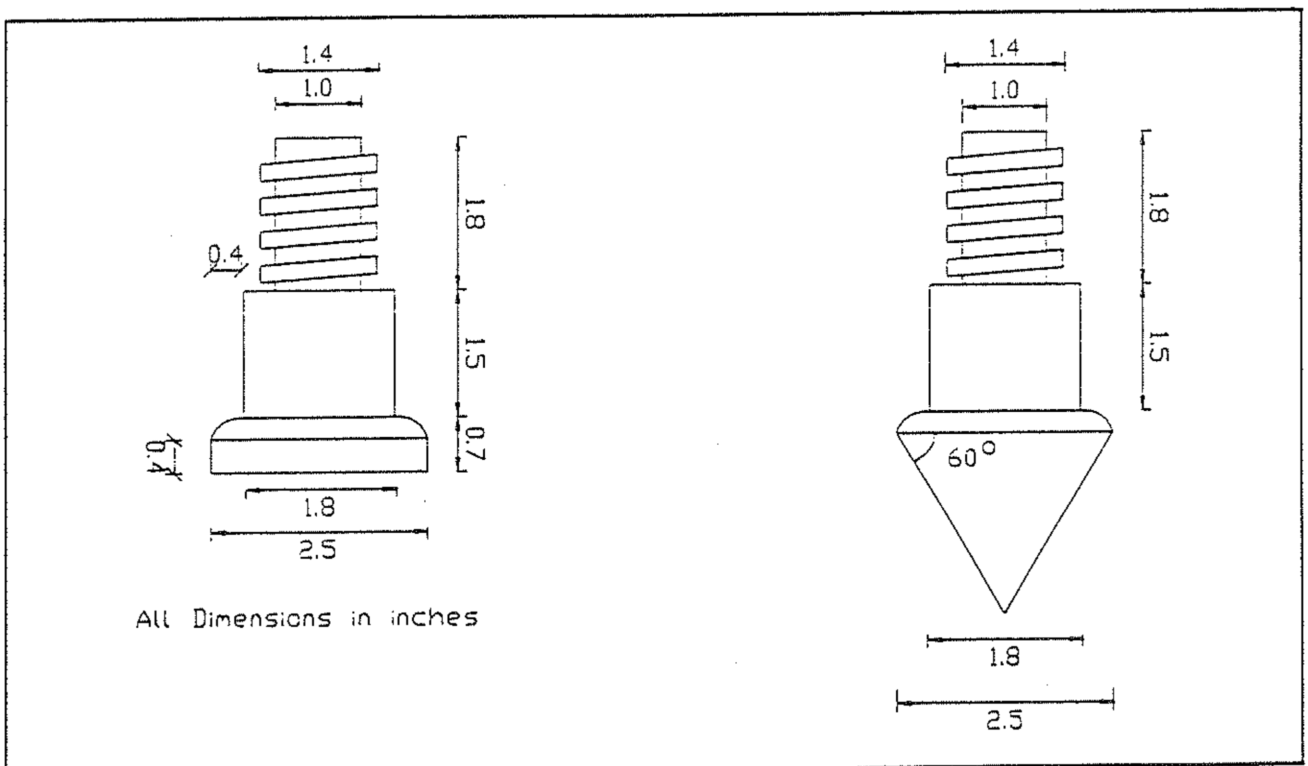

Figure 2: Oversized Tips - Flat End and Cone (1 inch = 25.4 mm)

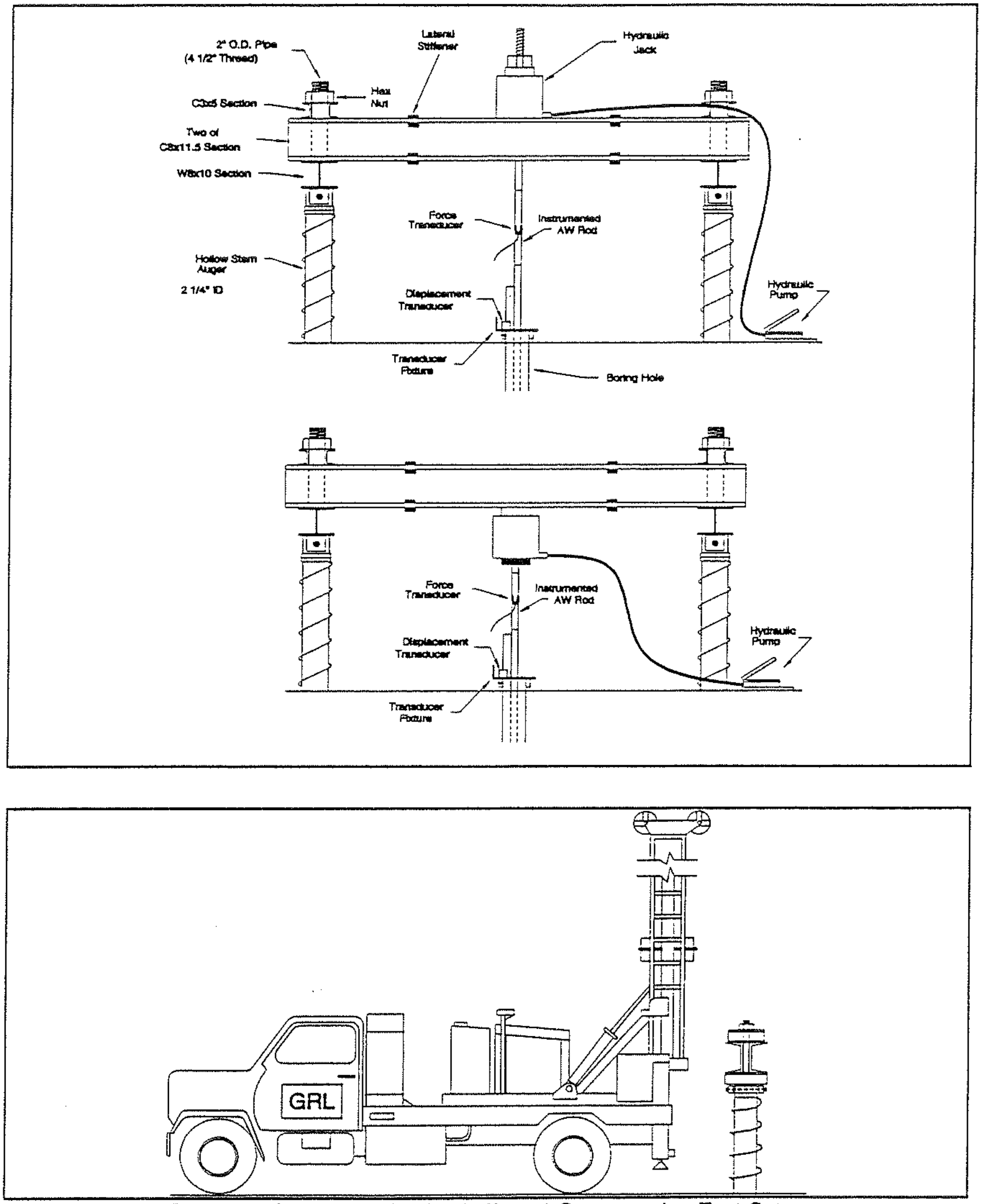

Figure 3: Schematic Static Uplift and Compression Test Setup

and hydraulic jack setup for uplift and compression test, respectively. The bottom figure shows the hollow stem augers and reaction frame setup with respect to the drilling truck. Figure 4a and 4b show the actual reaction frame setup for static uplift and compression test, respectively.

For static load measurement, the instrumented SPT rod for dynamic monitoring (Figure 2) was again employed. A commercial strain gage signal conditioner was used to balance and amplify the strain gage signals from the instrumented SPT rod, before the signal was fed into the data acquisition system. For displacement measurement, a fixture was mounted on the casing or hollow stem auger at the drill hole. Displacement transducers of a cable extension type, having a range of 10 inches (254 mm), were mounted on the fixture.

For several compression tests, depending on the drilling method, spacers were inserted in the drill rod connections at 10 ft (3 m) intervals to prevent drill string buckling. The spacers were effective when hollow stem augers or continuous casings were used in advancing the drill hole. However, in some cases, only drilling mud was used without casing and for those cases, the spacers were not considered useful and therefore not installed. Since the Modified SPT was designed to work with all drilling methods, no particular drilling method was prescribed. Several drilling methods were used in this study including hollow stem auger, continuous casing with water only, continuous casing with drilling mud, partial casing with drilling mud, and drilling mud only without casing.

Data Acquisition and Software for Static Test

Data acquisition of the static load test was also accomplished by a PDA, Model PAK. A special software called Automatic Load Test Program™ (ALTP) was developed which used the data acquisition in the PDA to record data. The program can be used for up to eight measurement channels. During a static load test, the program recorded the force and displacement data continuously and saved into the PDA's hard disk at a user specified frequency. The program displays the load *vs* displacement curve, the load and displacement time history, and the displacement rate on the PDA's screen during the static load test. Other optional features available in the program include the display of the Davisson's failure criterion, a transducer zero offset correction, and a pile weight correction. The displacement rate display in this program assisted the test engineer in maintaining a constant penetration rate. The pile weight option added the weight of the drill rod to the measured compressive load or subtracted it from the measured uplift load.

Torque Static Test

The torque tests were initially performed with a simple torque wrench which was capable of measuring torques up to 300 lbs-ft (406 N-m) with an accuracy of 5 lbs-ft (7 N-m). The torque results obtained from using the torque wrench were promising and therefore an instrumented torque rod was designed and manufactured by PDI. The torque rod was instrumented with foil gages. The torque was manually applied by a 4-foot (1.2 m) rod inserted into a "T" drive adaptor of a socket. The socket was mounted to the top of the torque rod (Figure 5). A torque test demonstration is shown in Figure 6.

The rotation due to torque was measured with the same displacement transducer and mounted on the same fixture for uplift and compression test. The displacement transducer was

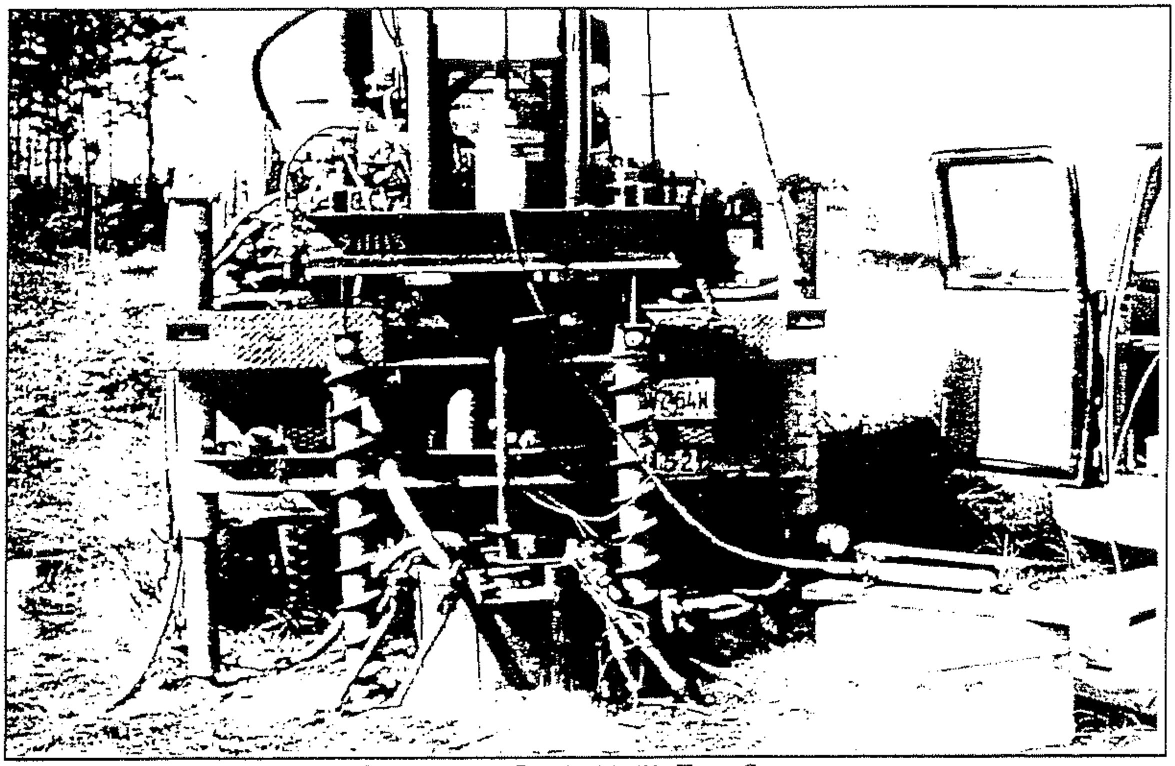

Figure 4a: Static Uplift Test Setup

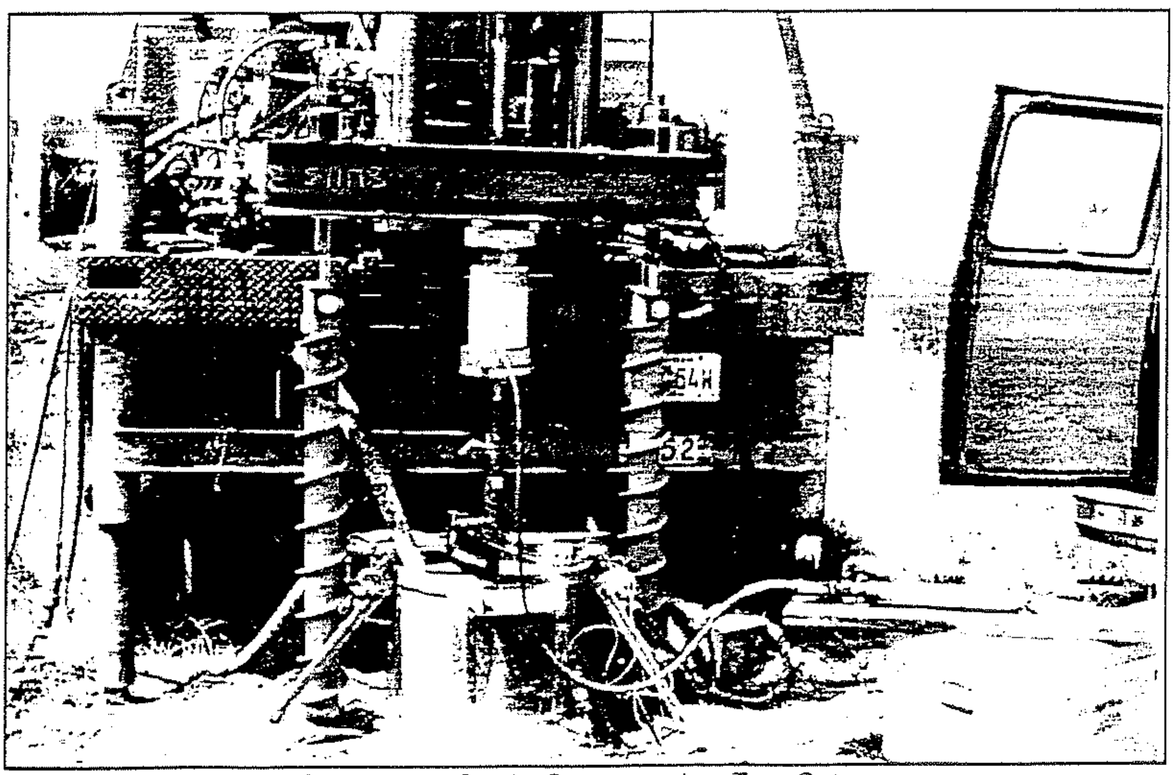

Figure 4b: Static Compression Test Setup

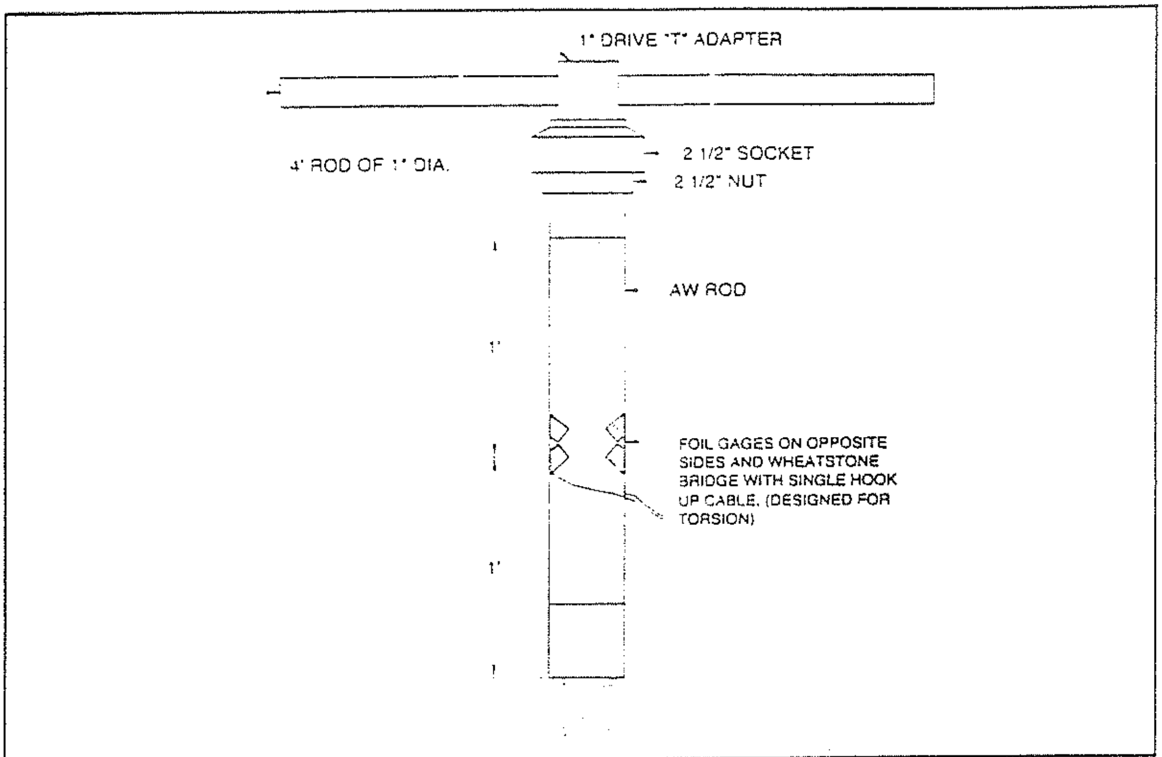

Figure 5: Instrumented Torque Rod (1' = 0.305 m; 1" = 25.4 mm)

Figure 6: Demonstration of Torque Test

positioned such that when the torque was applied, the transducer cable wrapped around the drill rod and measured the circumferential displacement. This displacement was later converted to angle of rotation. Both torque and rotation were automatically recorded by the PDA and ALTP program described above.

Instrumented Sampler

Force and velocity measured during SPT driving formed the basis for the calculation of dynamic soil parameters. Before these parameters can be determined, the bottom force and velocity at the sampler location must be calculated from the top measurements. The methods for calculating the bottom force and velocity from the top measurements have been discussed by Goble and Abou-matar (1992). To confirm that this calculation is correct, a split spoon sampler was instrumented with strain gages and an accelerometer to directly measure sampler force and velocity, respectively. Instrumentation added to the sampler was the same as that used for the rod top. Due to the time consuming and complicated nature of the test (*e.g.*, wire feeding through the rod and gage protection), sampler instrumentation was only attempted once. This one test proved the validity of the approach chosen. A comparison of directly measured sampler's force and velocity with those calculated from top measurements is shown in Figure 7.

STATIC SOIL PARAMETERS - ANALYSES AND RESULTS

Uplift and Compression

The static load test results were used in determining the soil unit strength (shear resistance and end bearing) and the flexibility (quake). The load *vs* displacement of most soils in uplift (shaft shear resistance) formed an "elasto-plastic" behavior which agreed with the Smith model assumption used in the wave equation analysis. Since the uplift load *vs* displacement of the SPT sampler in most soils behaved elasto-plastically, the unit shaft shear strength of the soil was determined from the maximum *pullout load*. The soil shaft quake was determined from the intersection of the initial tangent of the load *vs* displacement curve and the pullout load. The shaft quake values obtained from most uplift tests were generally quite small ranging from 0.03 to 0.06 inch (0.76 to 1.52 mm).

Unlike the shaft shear resistance, the compressive (end bearing) load *vs* displacement usually indicated some degree of strain hardening. As expected, this strain hardening effect was more clearly indicated in granular soils. Examples of SPT compression static load tests results for a clay and a sand soil type are presented as load *vs* displacement plots in Figure 8. In the case of sand in Figure 8, the load increased from 3.0 to 5.5 kips (13.3 to 24.4 kN) beginning where Davisson's criterion is reached to four inches (102 mm) of tip displacement. The unit end bearing was calculated by dividing Davisson's failure load by the tip area. The soil toe quake was not clearly indicated in the compression load *vs* displacement curves because of the strain hardening effect. Therefore, the toe quake was taken as the intersection between the initial tangent line through the origin and the horizontal line passing through the Davisson's failure load.

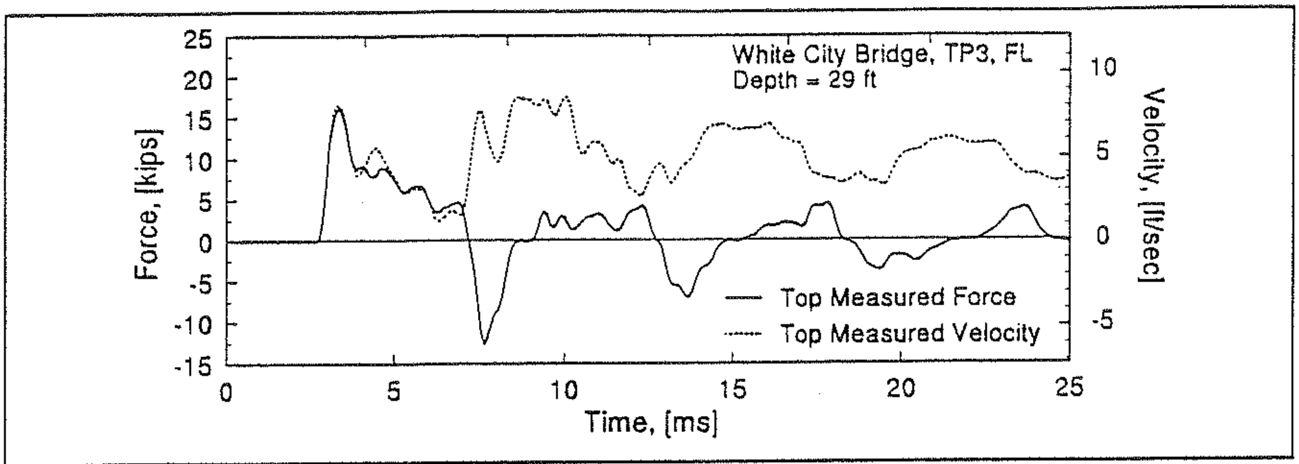

Figure 7a: Force and Velocity Measured at the Top (1 kip = 4.45 kN; 1 ft/s =0.305 m/s)

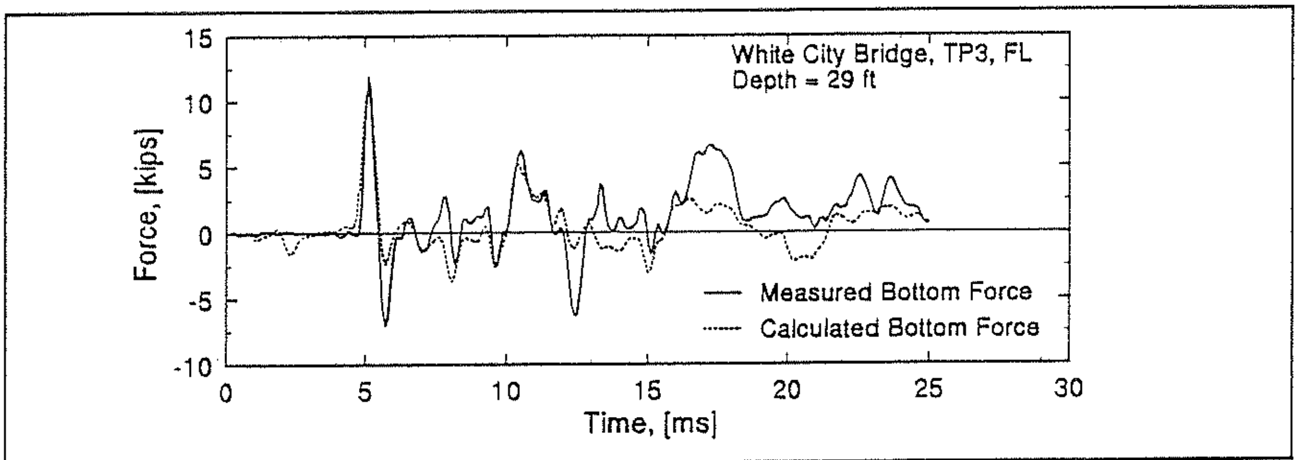

Figure 7b: Comparison Between Measured and Calculated Bottom Force

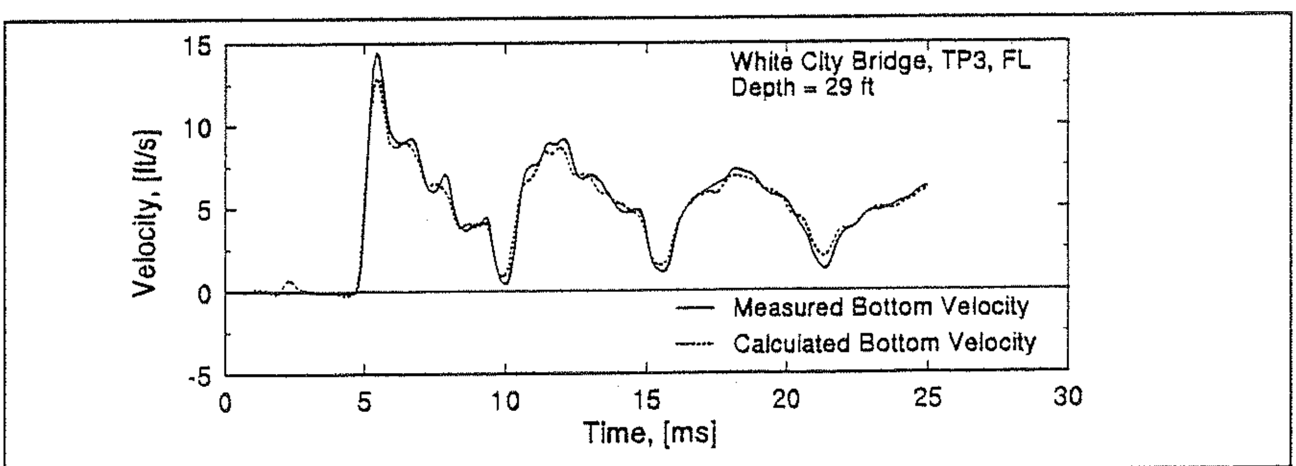

Figure 7c: Comparison between Measured and Calculated Bottom Velocity

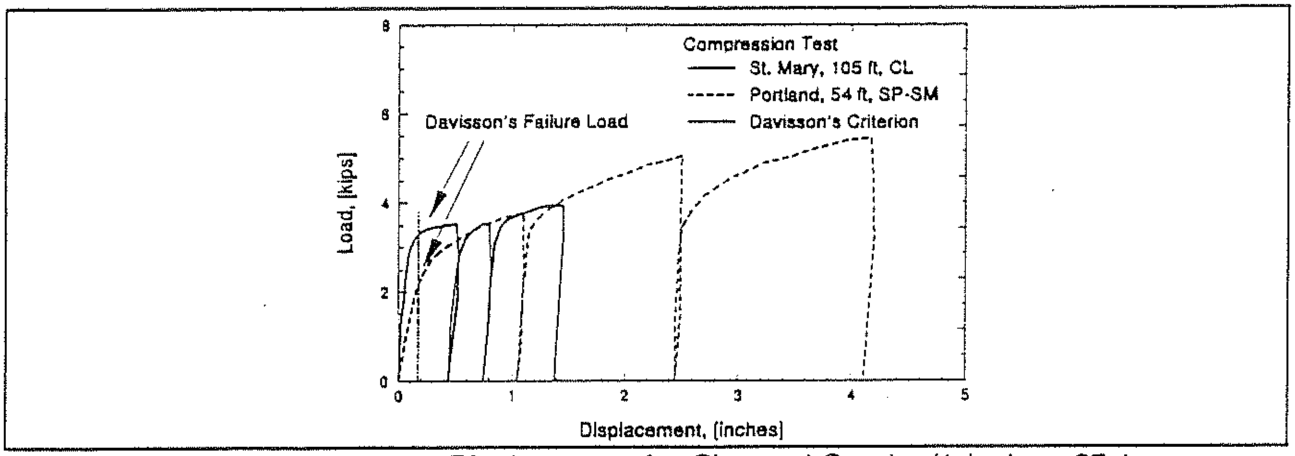

Figure 8: Typical Load versus Displacement for Clay and Sand (1 inch = 25.4 mm; 1 kip = 4.45 kN)

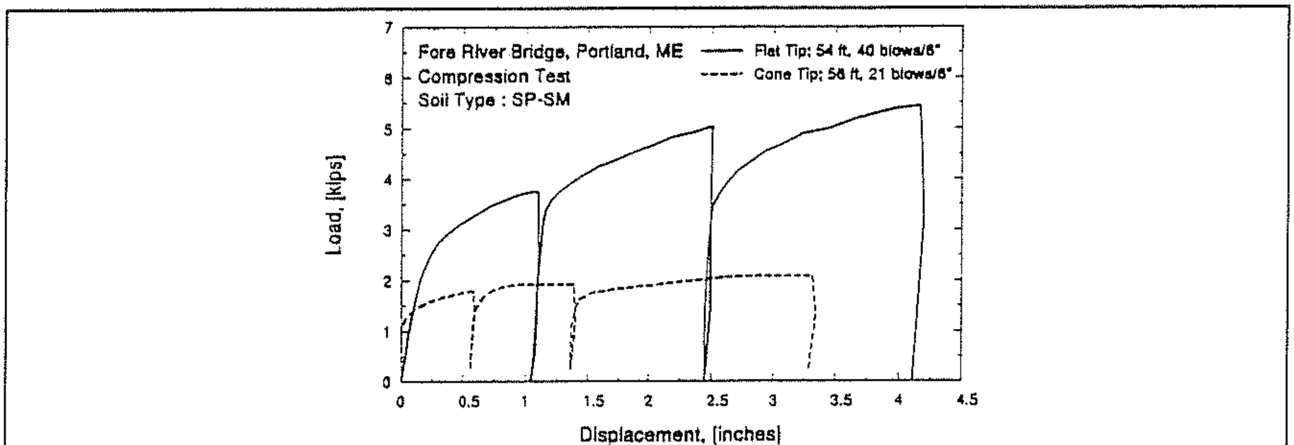

Figure 9a: Load versus Displacement for Flat End and Cone Tip at Portland Site

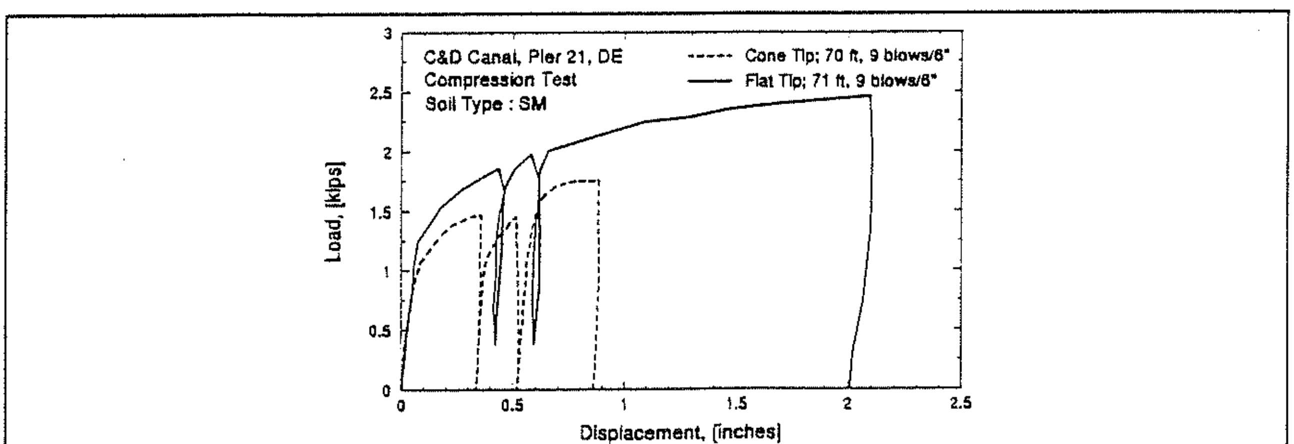

Figure 9b: Load versus Displacement for Flat End and Cone Tip at CD21 Site (1 inch = 25.4 mm; 1 kip = 4.45 kN)

Comparison of Flat and Cone Tip

Bearing behavior on two types of oversized SPT tips, having a flat end and a cone shaped tip have been investigated. Comparison tests between the performance of these two tips were conducted at two sites. At both sites, the tips were tested within 2 ft (0.61 m) depth to ensure a meaningful comparison. At one site, the flat end tip was used first followed by the cone tip; at the other site, the sequence was reversed to reduce the possibility of an incorrect conclusion due to loading history effects. The load *vs* displacement curves for both tip types and both sites are shown in Figures 9a and 9b.

Based on these two test results and considering several site and test specific conditions, it was concluded that the flat end tip indicated higher unit end bearings than the cone tip. The unit toe resistance predictions of the flat end tip at the Portland site appeared to agree more closely with the full scale test results than the cone tip. In addition, it appears that the flat end tip is more likely to detect soils with "large quake" behavior as observed on the full-scale pile. It was therefore decided to exclusively use the flat end tip at both the remaining test sites.

Scale Factor for Unit End Bearing Prediction

To evaluate the accuracy of unit end bearing predictions from flat end tip measurements, comparison calculations were made using unit end bearing from either a full scale pile static load test results or from CAPWAP results. The unit end bearing of the full scale pile can be calculated from the static load test results only when telltales or other load transfer measurements were made during the static load test. Only for two correlation sites (Portland and Apalachicola) did these measurements exist. CAPWAP based unit end bearing values were also correlated with SPT flat end tip measurements in the investigation. Figures 10a and 10b, show the unit end bearing *vs* displacement curves of the flat end tip together with the corresponding full scale load test curve. In addition, a scale factor was also calculated for agreement between the full scale pile curve and the flat end tip curve, and shown in the figures.

The unit end bearing *vs* displacement plots of scaled flat end tip and full scale pile load test with telltales showed good agreement. Unfortunately though, the required scaling factors were quite different: the Portland site required a scale factor of 2.1; for Apalachicola a scale factor of 0.56 had to be applied for agreement. The respective soil types were granular and cohesive. Further evaluation of six sites which had the CAPWAP calculated unit end bearing values and flat end tip measurements indicated, however, that a scaling factors less than or equal to one. At the present, it must be concluded that the end bearing predictions from flat end tip measurements could be 1/2 to 2 times of the full scale pile result.

Rate Effect of Soil Resistance

Several investigators (Coyle and Gibson, 1970; Litkouhi and Poskitt, 1980; and Heerema, 1981) have found that dynamic resistance is not linearly but exponentially related to the rate of loading. To check this hypothesis, static compression and uplift tests were conducted at different rates. Unfortunately, the investigation of rate effect on flat end tip compression loading was not successful because loading history also had a profound effect on the end bearing capacity. Thus, several cycles of loading would always produce different capacity values regardless of loading rate. Therefore, the rate effect study was concentrated on the shear loading from uplift

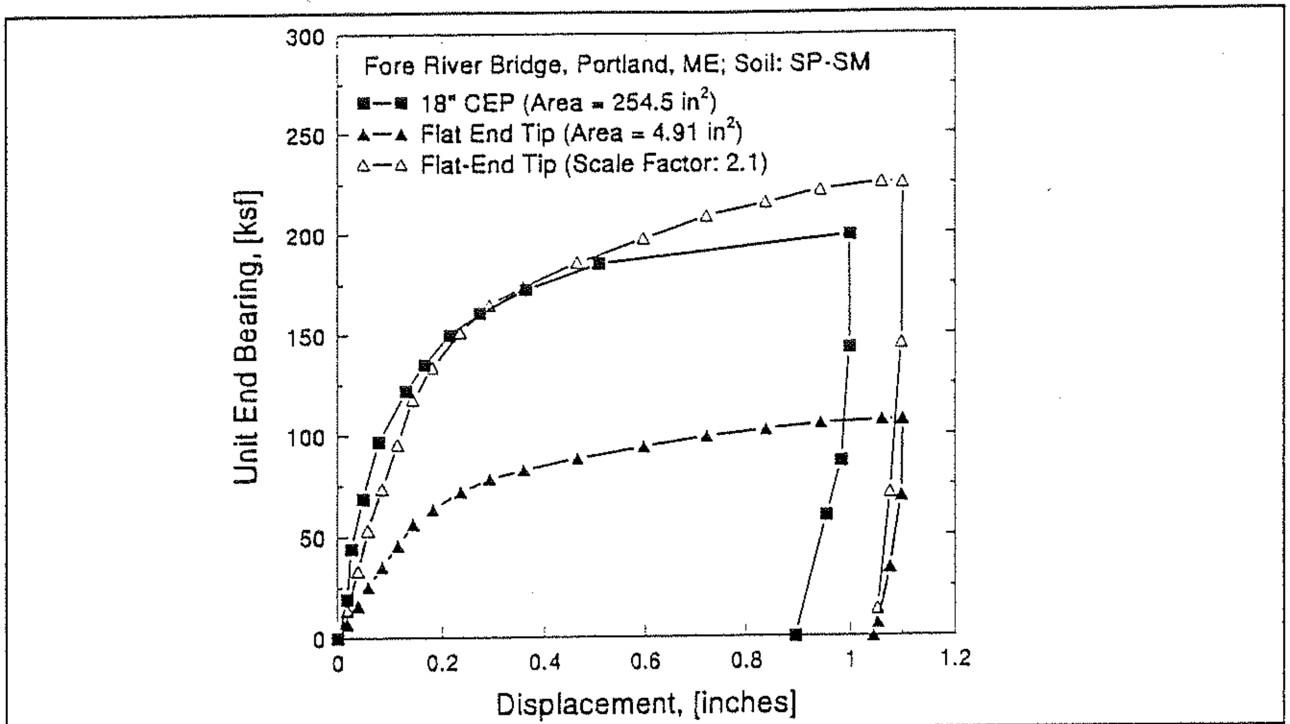

Figure 10a: Load versus Displacement for Flat End Tip and Full Scale Pile, Portland Site (1 inch = 25.4 mm; 1 ksf = 48 kPa)

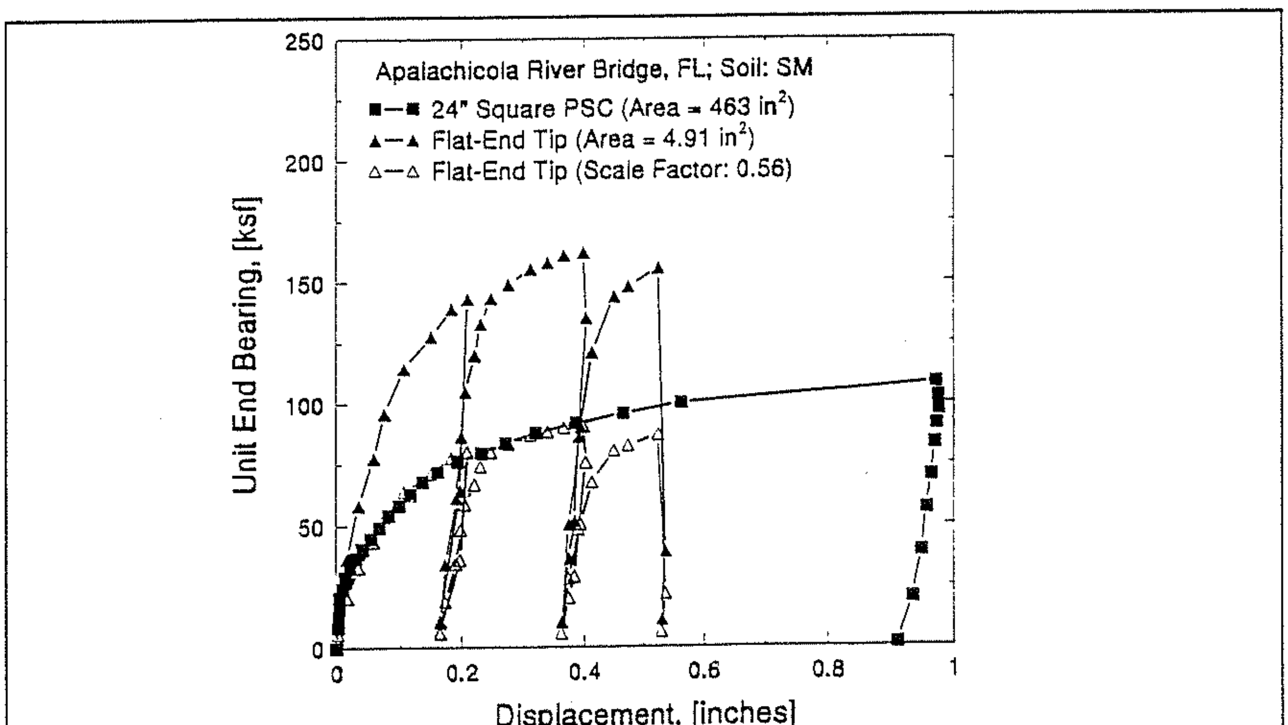

Figure 10b: Load versus Displacement for Flat End Tip and Full Scale Pile, AP Site (1 inch = 25.4 mm; 1 ksf = 48 kPa)

test of the sampler which were typically conducted at rates between 0.01 inches per minute (.25 mm/min) and 1.8 inches per minute (45.7 mm/min).

Since higher displacement rates could not be achieved by the static uplift test, another approach was attempted. In this case, several different hammer drop heights, varying from 2 to 30 inches (51 to 762 mm), were used to generate different impact velocities and therefore different sampler velocities. The sampler was first driven 18 inches (457 mm) and the SPT N-value was 2. The sampler was then left in the soil for about 15 hours to allow for soil setup, before various hammer drop heights were applied. The force and velocity time histories at the sampler resulting from various hammer drop heights, are presented in Figure 11a and 11b. The peak forces (resistance) and peak velocities from different hammer drop heights were then evaluated in a regression analysis to yield damping factor, J_C, and exponent, n, of Coyle's dynamic resistance equation:

$$R_d = R_s \, [1 + J_c \, \dot{u}^n] \tag{1}$$

where R_d is the total dynamic resistance; R_s is the static resistance; and $\dot{u}$ is the velocity of the sampler. The main objective of this study was to determine the value for n.

By using regression analyses of the results from uplift test, the value for n were found to be between 1.07 and 1.24, with the corresponding J_C values of between 2.17 and 3.19 $(s/ft)^{1/n}$. For the study with different hammer drop heights, the exponent and damping factor from the regression analysis were $n = 0.916$ and $J_C = 1.81$ $(s/ft)^{1/n}$, respectively. Figure 12 shows the resistance *vs* logarithmic velocity plot together with the best fit line from which the exponent and damping factor were determined. The n values indicated in these studies did not differ much from unity and therefore did not suggest that the traditional Smith approach was inadequate.

Soil Setup

Soil strength changes with time or soil setup following the end of pile driving has been a well recognized phenomenon in the piling industry. Static uplift tests from three different sites were used to study the soil setup (Apalachicola, Aucilla and Vilano West.) Results from eight uplift tests, performed at various depths, were available. At each test location, the uplift test was performed at the end of sampler driving, after a 15-minute and a 1-hour wait. At two test locations, an 11 and 14-hour wait were also performed. The soil type at these three sites was generally cohesive or between MH and OH according to the USCS Classification system. The SPT N_{60} [2] values were very low, ranging between 1 and 5. Atterberg tests indicated that the Liquid Limits of these soils were between 65 and 94%, the Plastic Limits were between 28 and 53% corresponding to Plasticity Indices between 31 and 66%. This soil type is considered to be of medium to high plasticity. For this study, the generally accepted theory that soil strength gains logarithmically with time (Skov and Denver, 1988) was tested. For simplicity, the initial uplift soil shear strength was assigned a waiting time of 1 minute. The data from each test location was then plotted in Figure 13 along a logarithmic waiting time scale.

---

[2] N_{60} is an SPT N value corrected for transferred energy variations from the perceived average of 60%. The correction is based on dynamic measurements during the Modified SPT.

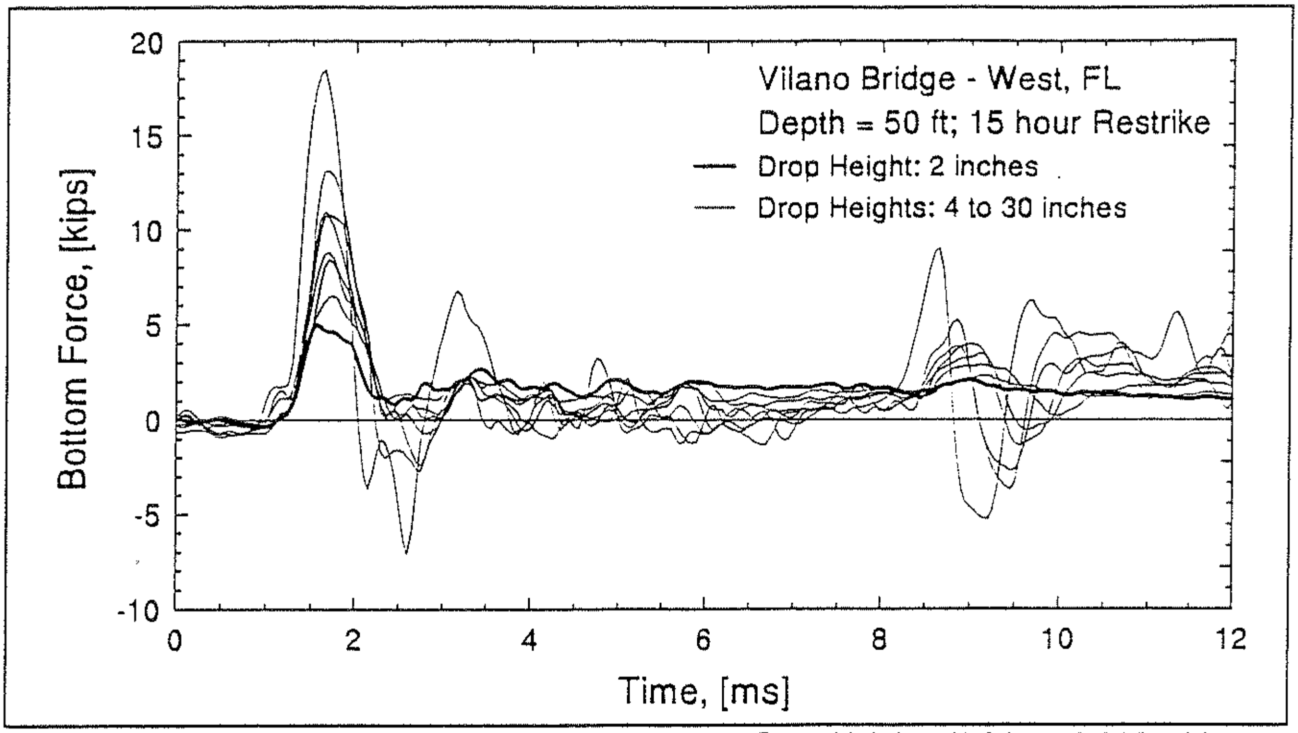

Figure 11a: Bottom Force from Various Hammer Drop Heights (1 ft/s = 0.305 m/s)

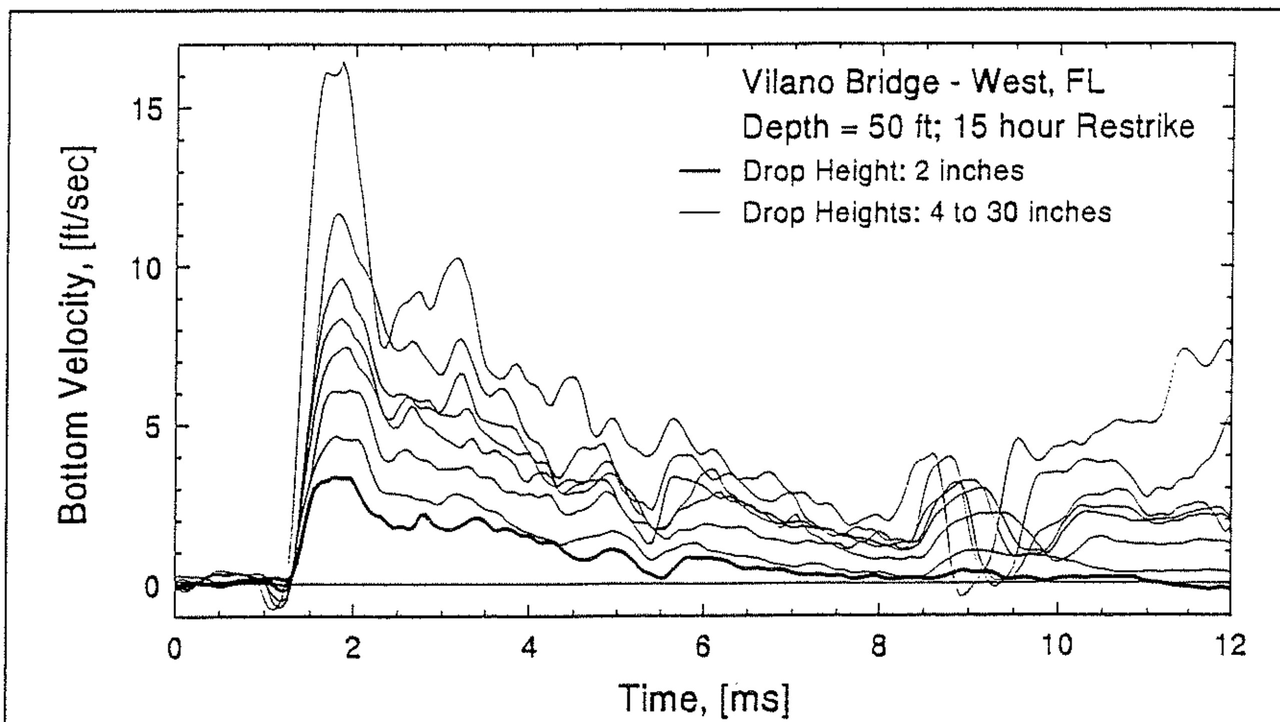

Figure 11b: Bottom Velocity from Various Hammer Drop Heights (1 kip = 4.45 kN)

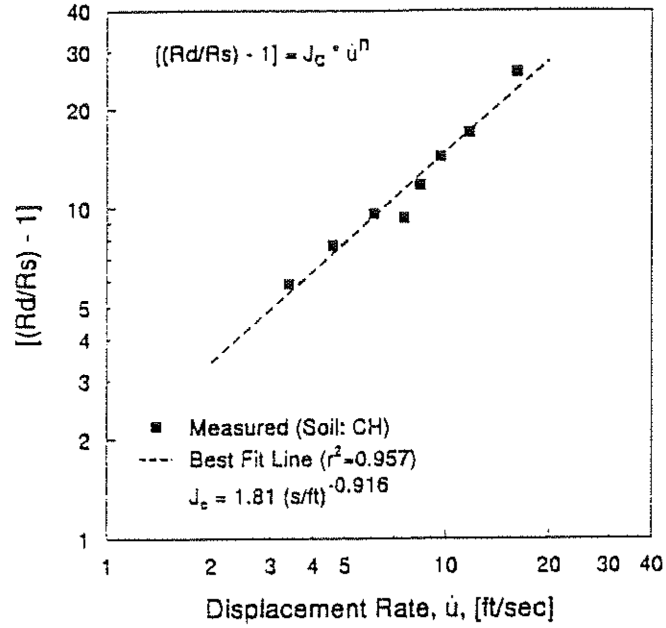

Figure 12: Rate Effect Study for CH Type Soil (1 ft/s = 0.305 m/s)

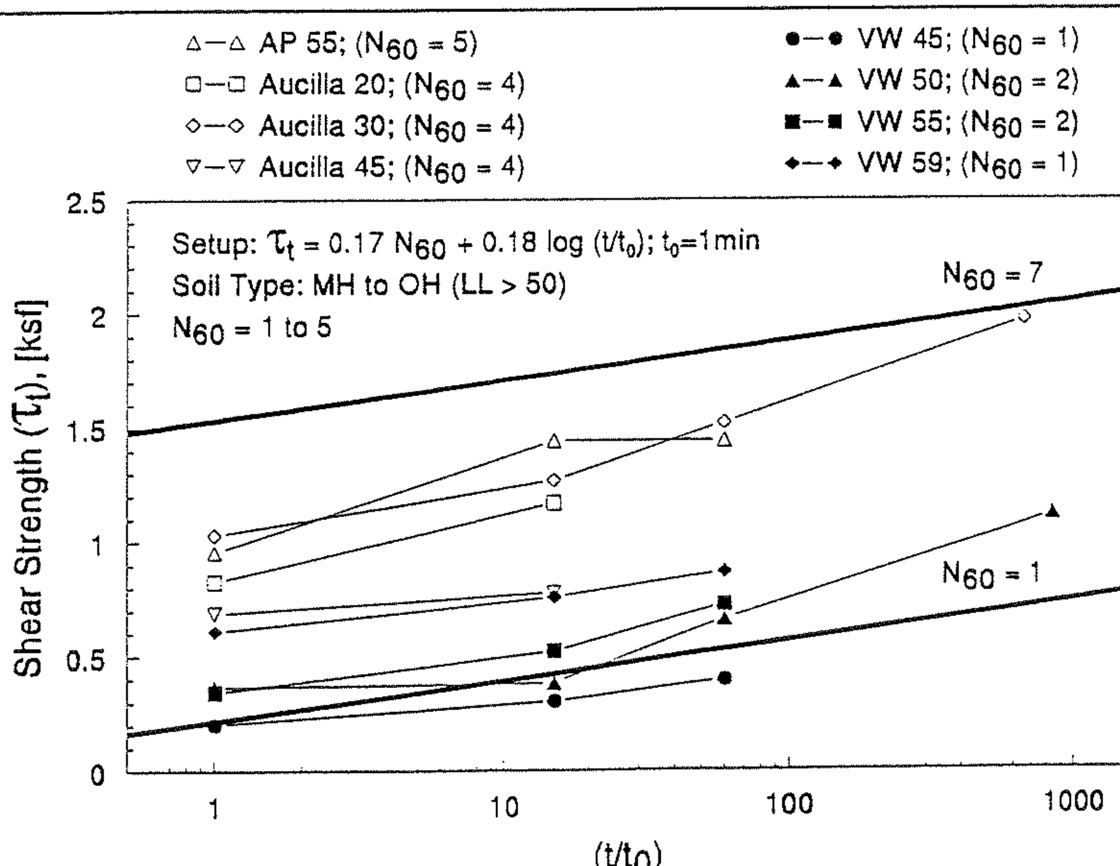

Figure 13: Setup Evaluation for Three Sites (1 ksf = 48 kPa)

Another study involved full scale pile test results of the Apalachicola site. There dynamic testing and CAPWAP analyses were performed both during the end of driving and at the beginning of restrike, immediately following the static load test. The capacity predicted by CAPWAP utilizing the radiation soil model agreed well with the static load test result. The CAPWAP results also indicated that the end of driving and beginning of restrike pile shaft resistances were 184 and 520 kips (817 and 2309 kN), respectively, yielding a setup factor of 2.83. The time between the end of driving and the beginning of restrike was 12 days or 17,280 minutes. Using the relationship indicated in Figure 13 the setup factor would be estimated at 2.40.

Torque Tests

In addition to and following the uplift test, the torque test was performed to determine the shear strength of the soil prior to split spoon sampler extraction. The torque generates a horizontal shear loading between the outside perimeter of the split spoon sampler and the soil. The torque resistance is calculated by dividing the measured torque by the radius of the sampler. The torque resistance divided by the embedded sampler shaft area yields the unit torque resistance.

A total of 20 torque tests were performed during this investigation. In some uplift tests, the load-displacement curves indicated both a peak and a residual strength. At most of the torque test sites, an uplift test was performed prior to the torque test. The uplift test was also repeated approximately 15 minutes to 2 hours after the end of sampler driving.

Comparisons of unit torque and uplift resistances are presented in Figure 14 together with the soil setup factor from uplift tests performed after various waiting times and a general description of soil types at the test sites. Figure 14 shows both the peak and residual torque resistances and also indicates the range of uplift resistances. At site F, a Shelby tube sample was extracted and an unconfined compression test was performed on the sample. The unconfined compression strength of the sample is also presented in Figure 14 for comparison with the torque and uplift resistance together with a general description of soil types at the torque test sites. Please note that the order of test locations in Figure 14 follows the magnitude of the ratio of peak to residual torque resistance.

In general, the results show good agreement between torque and uplift resistance. The uplift resistance generally falls between peak and residual torque, indicating that the uplift resistance may be determined by factoring either one of these two values. Figure 15 is a scattergram of uplift resistance *vs* peak torque and includes the best fit regression line indicating that uplift resistance including setup averages 69% of the peak torque resistance.

DYNAMIC SOIL PARAMETERS - ANALYSES AND RESULTS

Evaluations of the dynamic soil parameters (damping and quake) from the measured dynamic records were more complex than the evaluation of static soil parameters from static tests. Basically two approaches were investigated. In the first approach, the measured dynamic records were matched by performing wave equation analyses of the SPT driving system using GRLWEAP. The second approach employed a direct signal matching procedure.

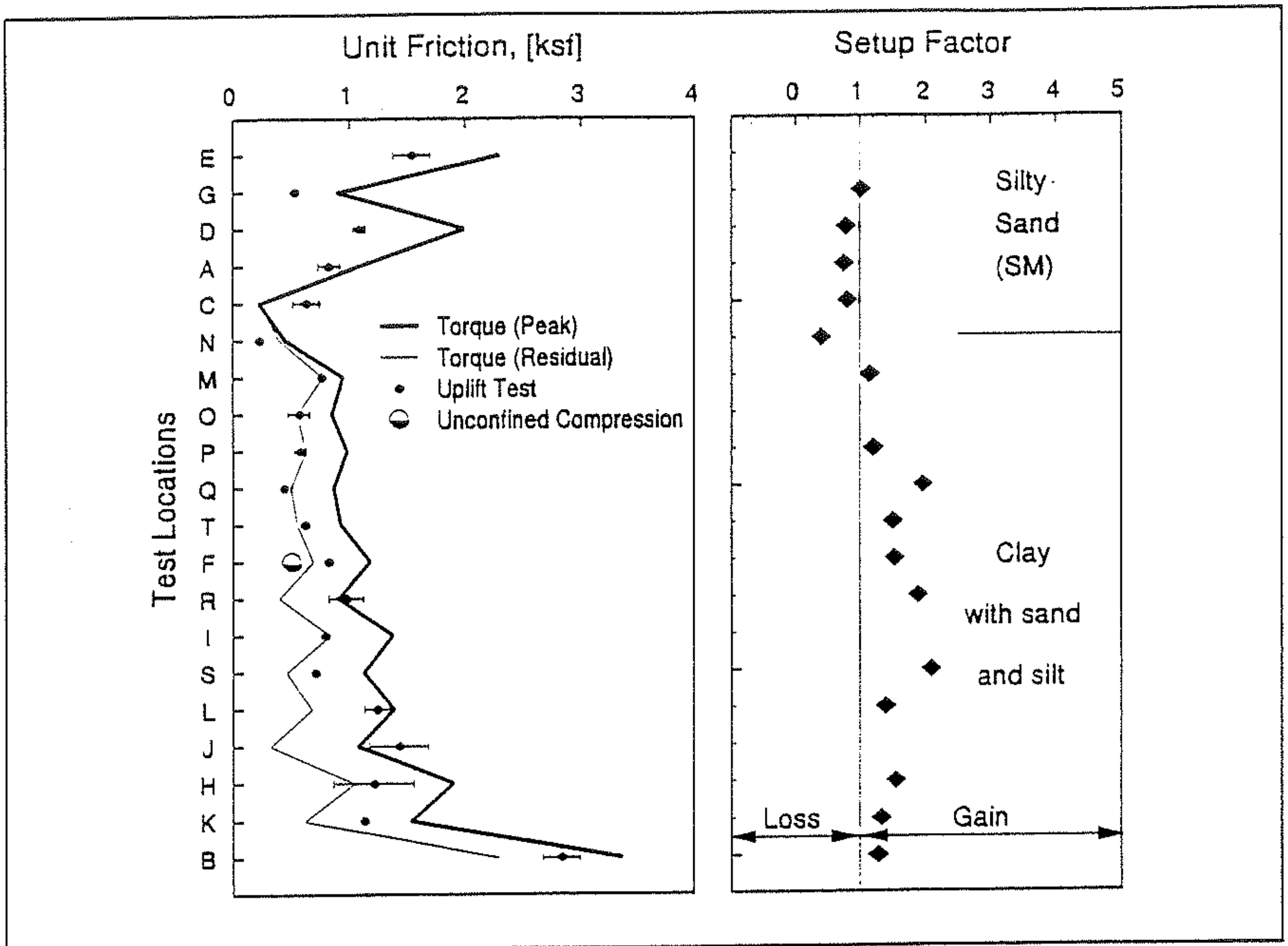

Figure 14: Summary of Torque Test Results from 20 Sites (1 ksf = 48 kPa)

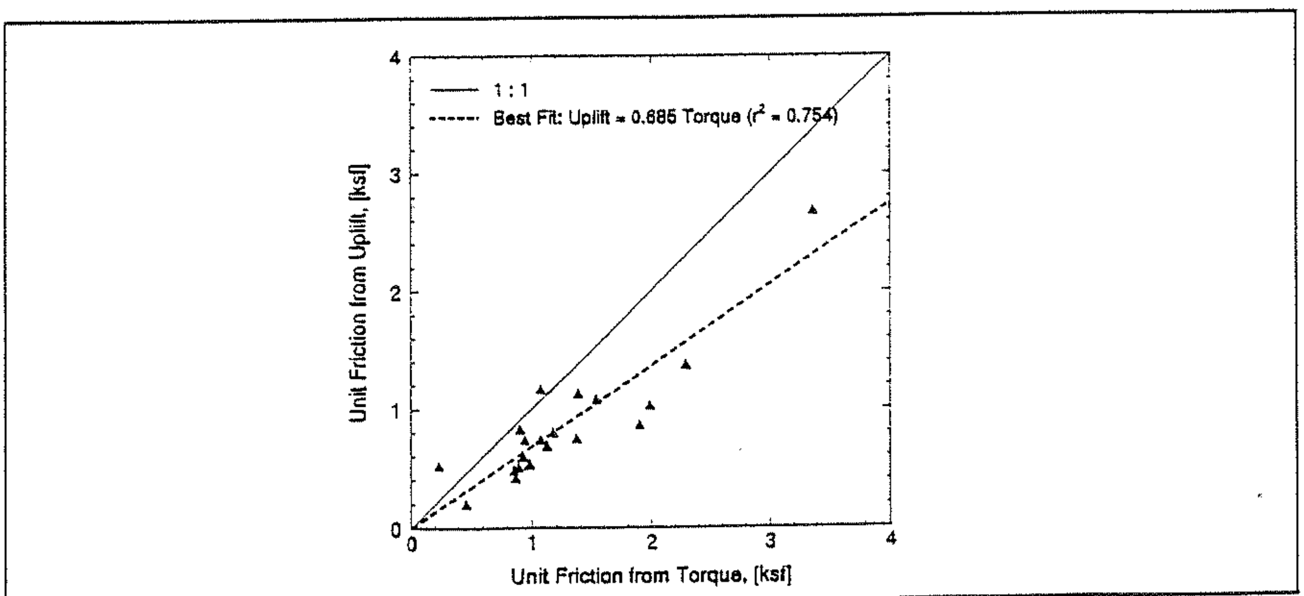

Figure 15: Torque Resistance vs Uplift Resistance (1 ksf = 48 kPa)

GRLWEAP Matching

Both top and bottom records from GRLWEAP and measured dynamic records were compared as shown in Figure 16a and 16b, respectively. The bottom records were obtained from the measured top records by simple wave mechanics as explained by Goble and Abou-matar (1992). The bottom records thus calculated were referred to as the *"measured"* quantities when they were compared with the calculated values from wave equation.

Complications in the comparison arose only when the measurements included reflections from open (loose) connectors. Then the wave speed of the rod was affected and was different in tension and compression. The so-called bottom measurements were then rather inaccurate. However, for most cases, the basic approach of calculating "measured" bottom quantities from top measurements was a sound one as shown by the verification measurements presented in Figure 7.

The good match between the measured and calculated top force and velocity (Figure 16a) indicates a good GRLWEAP pile model. The good match between the measured and computed bottom force and velocity (Figure 16b) suggests that the Smith soil model incorporated in GRLWEAP is adequate to predict the shaft behavior. The adequacy of the Smith shaft soil model can be further demonstrated by plotting the dynamic force versus the dynamic displacement records together with the static load *vs* displacement curve as shown in Figure 17. This figure indicates how dynamic records can be very simply evaluated for static and dynamic model parameters.

As discussed earlier, the static compression resistance of granular soil indicated significant strain hardening. This strain hardening behavior also occurred during the dynamic loading and was not represented by Smith's elastic-perfectly plastic soil model. Such strain hardening behavior was successfully modeled using two quakes parameters, one defining the initial slope of the load-set curve and one at which failure was reached, forming a hyperbolic (Rausche, et al., 1994). This new soil model was incorporated in GRLWEAP and was used to match the measured bottom force and velocity. Comparisons between the measured and GRLWEAP calculated dynamic force versus dynamic displacement plot, and also with the static load *vs* displacement plot for cohesive and granular soil are presented in Figures 18 and 19, respectively. Figure 18 shows that the Smith's toe soil model is adequate for cohesive soil. However, for granular soil a better match was obtained with the hyperbolic soil model as shown by Figure 19.

Dynamic Signal Matching

This procedure again required the calculation of the "measured" bottom force and velocity. Bottom displacement and acceleration were obtained by integrating and differentiating the bottom velocity, respectively. Thus, the inertia resistance components due to sampler and/or soil plug weight, damping resistance and static resistance components could be calculated for an assumed set of mass, damping factor, quake and R_u. The resulting resistance force was compared with the "measured" one. Adjustments were then made to the resistance parameters for an improved match. The dynamic signal matching method has been discussed in detail by Goble and Abou-matar (1992).

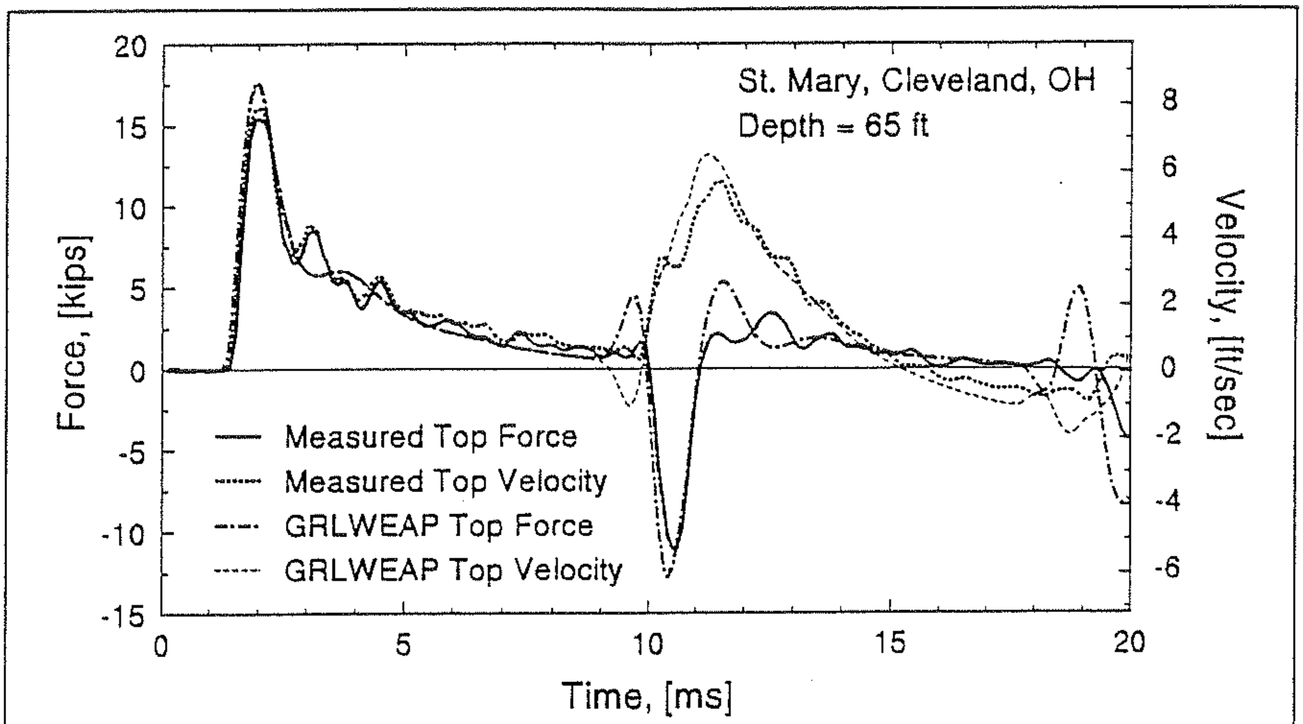

Figure 16a: Comparison Between GRLWEAP and Measured Top Force and Velocity (1 kip = 4.45 kN; 1 ft/s = 0.305 m/s)

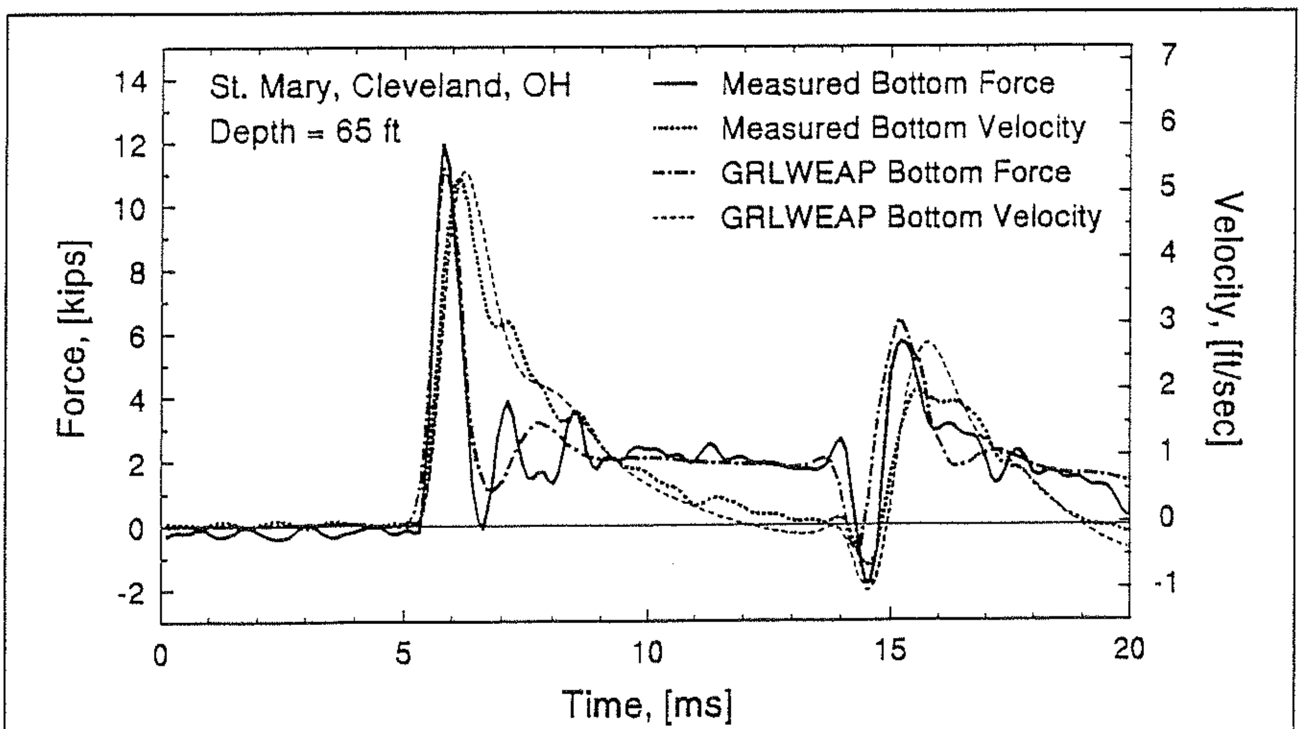

Figure 16b: Comparison Between GRLWEAP and Measured Bottom Force and Velocity

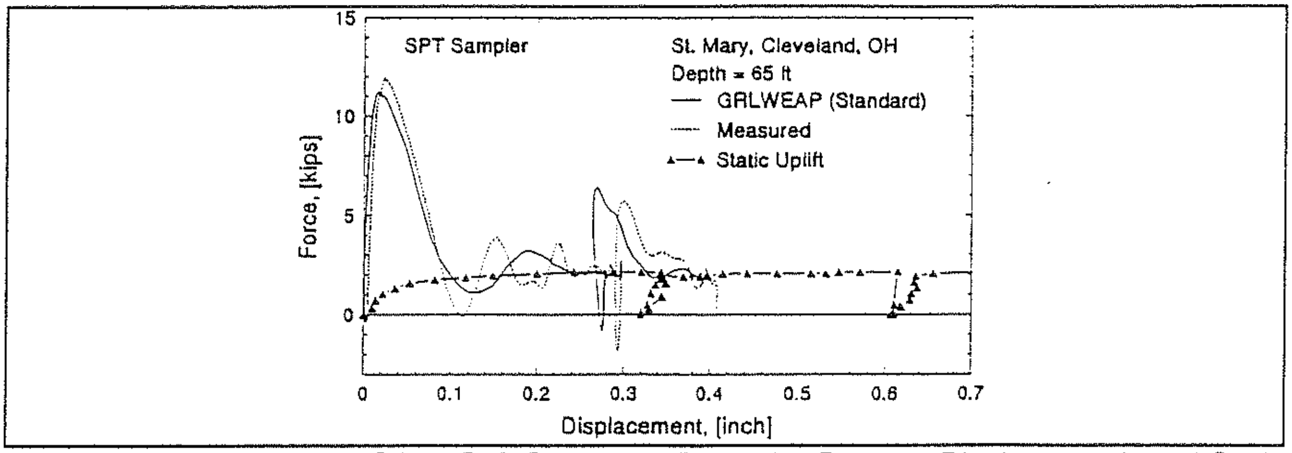

Figure 17: Measured and GRLWEAP Computed Dynamic (Force *vs* Displacement), and Static (Force *vs* Displacement) for Shaft Resistance (1 kip = 4.45 kN; 1 inch = 25.4 mm)

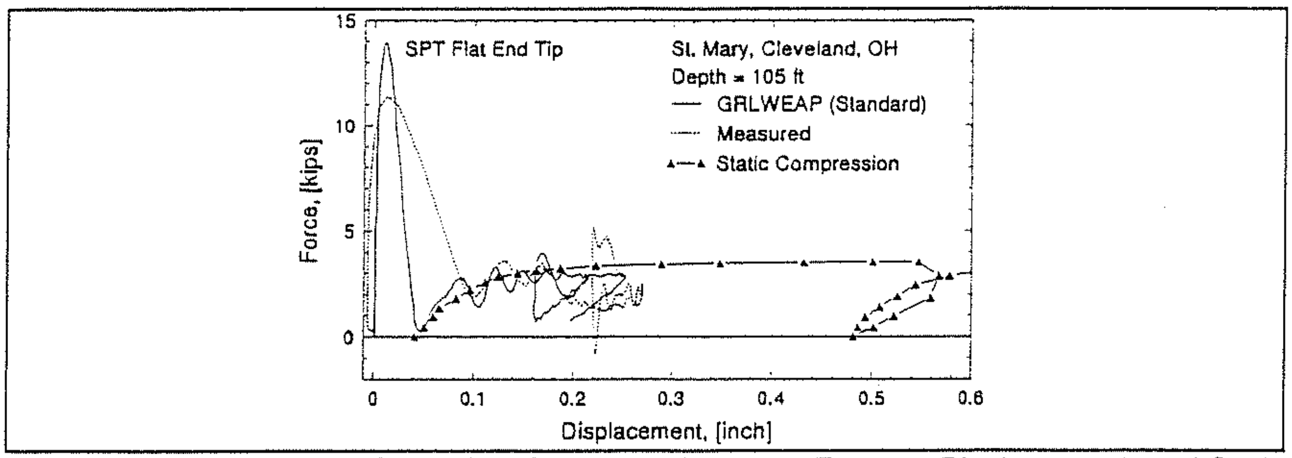

Figure 18: Measured and GRLWEAP Computed Dynamic (Force *vs* Displacement), and Static (Force *vs* Displacement) for Flat End Tip on Cohesive Soil

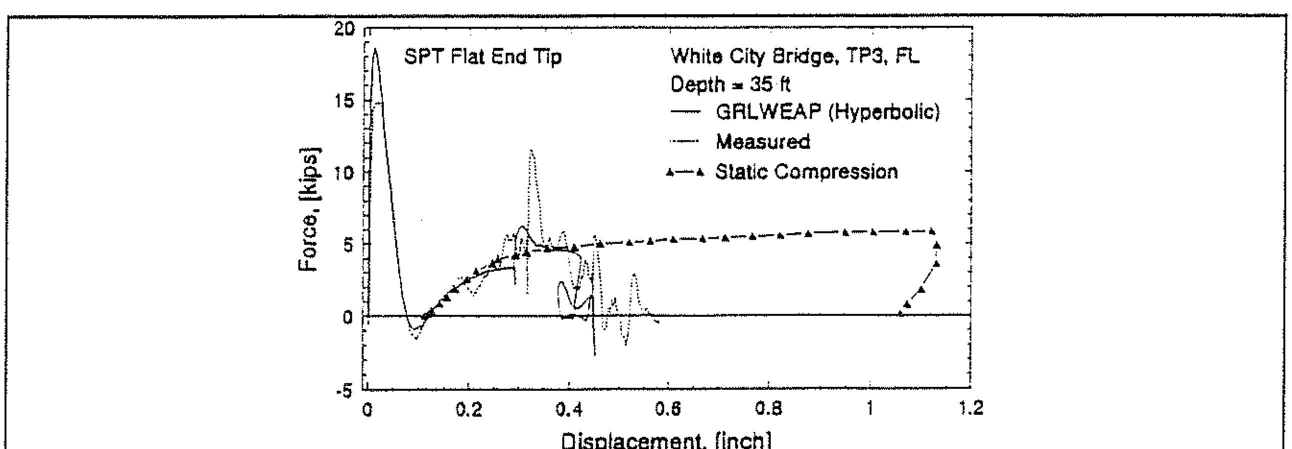

Figure 19: Measured and GRLWEAP Computed Dynamic (Force *vs* Displacement), and Static (Force *vs* Displacement) for Flat End Tip on Granular Soil

There are two ways for calculating the matching quantity. For example, the CAPWAP type method which attempts to find three parameters: static resistance, R_u, quake, q, and damping parameter, J, from the optimal agreement between the "measured" and computed sampler quantities, force and velocity. A second method, perhaps the most logical one given the static measurements, would calculate the computed force using the known R_u and q values from pull-out or compression test and J from the signal matching. Obviously, this method tacitly assumes that the static resistance is the same during dynamic and static event. Unaccounted for setup effects could cause an error in the damping parameter determination.

BEARING GRAPH AND DRIVABILITY

Once the soil parameters have been calculated bearing graphs and drivability blow counts can be calculated for the full scale load test piles. Capacity predictions are taken from the bearing graphs (note that the static resistance values from SPT were not merely summed for capacity predictions; instead the wave equation approach plus the observed blow count were used for the prediction of capacity). Several combinations of parameter calculation methods can be employed and in all, six different methods were tried and compared as follows.

SPT-ST: (SPT Static); the Modified SPT static uplift and compression test values, R_u and q; damping parameters from dynamic signal matching with known R_u and q.

STD-ST: (Standard and static); Static resistance from Modified SPT, and soil model parameters according to GRLWEAP manual.

MDF-ST: (Modified Static); As for STD-ST but with toe damping factors fixed at relatively low values as suggested by dynamic signal matching.

SPT-DYN: (SPT dynamic matching); all resistance and soil parameters from dynamic signal matching.

MDF-Cap SPT: (Modified Capacity + SPT); static resistance values from pile static load test; quakes from Modified SPT static tests; damping from dynamic signal matching with known R_u and q.

MDF-Cap STD: (Modified Capacity + Standard GRLWEAP); static resistance values from pile static load test plus standard GRLWEAP soil parameters.

Except for the MDF methods, for bearing capacity predictions or correlations with a full scale load tests, the end bearing parameters were taken from SPT compression tests used from a comparable depth and several SPT test locations along the shaft were evaluated for shaft resistance values.

For drivability predictions, end bearing also had to be calculated for several locations along the pile shaft. Since the special tests were not conducted at all locations where samples were taken, the standard penetration N values were used to prorate results from locations with special tests. The SPT N-values were adjusted for energy fluctuations.

Table 2 summarizes the GRLWEAP capacity prediction using all six parameter combinations. Load test capacities and standard GRLWEAP results (based on the restrike blow count) are also included. The table also gives a brief highlights of the method features. For three different test piles, complete results from a number of these methods are also depicted in a bearing graph type presentation in Figures 20, 21, and 22.

Drivability predictions were also based on the above six parameter combination. These results were plotted in the form of blow counts *vs* depth in Figures 23, 24 and 25 for the above three test piles.

Based on these results, it was felt that the MDF-ST yielded the most reliable prediction of capacity and blow counts. This method relies on the Modified SPT static results, the present GRLWEAP shaft damping parameters and relatively small toe damping values which had been obtained by signal matching of special tip dynamic measurements.

CONCLUSIONS

The investigation described in this paper could be considered a feasibility study in the use of the Modified SPT for the prediction of pile driving behavior. The findings of this research support the following conclusions.

Clearly the greatest effort in this study was devoted to the development and first application of test equipment for the Modified SPT, to the performance of the test, and to the calculation of static and dynamic resistance parameters for full scale piles based on the Modified SPT results. On nine sites the Modified SPT was performed: static load test piles had prior been installed and tested on six sites, while on three sites, static and dynamic tests were to be performed later.

The Modified SPT included both static and dynamic measurements during and after the standard sampler driving without affecting the N-values measured. The dynamic measurements included hammer impact velocity, force and velocity during sampler driving and during driving of the rod with a special tip. The sampler was statically uplift tested at various extraction rates and after a variety of waiting times. Additional shaft unit resistance values were calculated from torque tests. The special tip equipped rod was also statically compression tested yielding load-displacement curves.

It was concluded that a flat end tip would produce results better comparable with full scale pile toe behavior than cone tips which had a lower end bearing and quake. The flat end tip indicated a very realistic post failure strain hardening behavior in granular soils. This information could be used for better load-set predictions and more economical failure criteria definitions.

It was also concluded that the simple torque test gave unit shaft resistance values which agreed well with those from uplift. Thus, the Modified SPT can be simplified.

It was found that the unit end bearing could be determined from the toe resistance of the sampler; and therefore, the special tip test might be replaced with a compression test on the sampler itself. This is especially true in those frequent cases where shaft resistance is negligible

Table 2: Comparison of Capacity Predictions from Dynamic SPT, GRLWEAP, and Static Load Test

Pile	Load Test [kips]	Standard GRLWEAP [kips]	SPT-ST [kips]	MDF-ST [kips]	STD-ST [kips]	SPT-DYN [kips]	MDF-Cap SPT [kips]	MDF-Cap STD [kips]
St. Mary	315	370*	410	350	340	310	--	340
Portland, ME	350	470*	160	325	210	160	150	210
C&D 17	1150	1240*	1250	1350	1150	1350	1050	1150
C&D 21	1300	1700*	2000	1350	1300	2000	2020	1350
White City	630	675*	690	690	510	540	--	510
Apalachicola	958	1015*	1110	1120	1115	1060	1115	1030
Ratio to Load Test		1.06-1.34	0.46-1.54	0.93-1.17	0.60-1.16	0.46-1.54	0.43-1.55	0.60-1.08
Average		1.17	1.11	1.08	0.94	1.02	1.01	0.93

Method Description

Source of	SPT-ST	MDF-ST	STD-ST	SPT-DYN	MDF-Cap SPT	MDF-Cap STD
Static Resistances	SPT Static Uplift Tests	SPT Static Uplift Tests	SPT Static Uplift Tests	SPT Dynamic Matching	Pile Load Test	Pile Load Test
Shaft Damping	SPT Dynamic Matching + Uplift (R_u, q)	GRLWEAP	GRLWEAP	SPT Dynamic Matching	SPT Dynamic Matching + Uplift(R_u, q)	GRLWEAP
Toe Damping	SPT Dynamic Matching + Comp. (R_u, q)	.005 to .08 s/ft (.016 to .262 s/m)	GRLWEAP	SPT Dynamic Matching	SPT Dynamic Matching + Comp. (R_u, q)	GRLWEAP
Quakes	SPT Static Tests	SPT Static Tests	GRLWEAP	SPT Dynamic Matching	SPT Static Tests	GRLWEAP

Notes: * Based on Restrike Test Results; 1 kip = 4.45 kN.; Comp. - Compression.

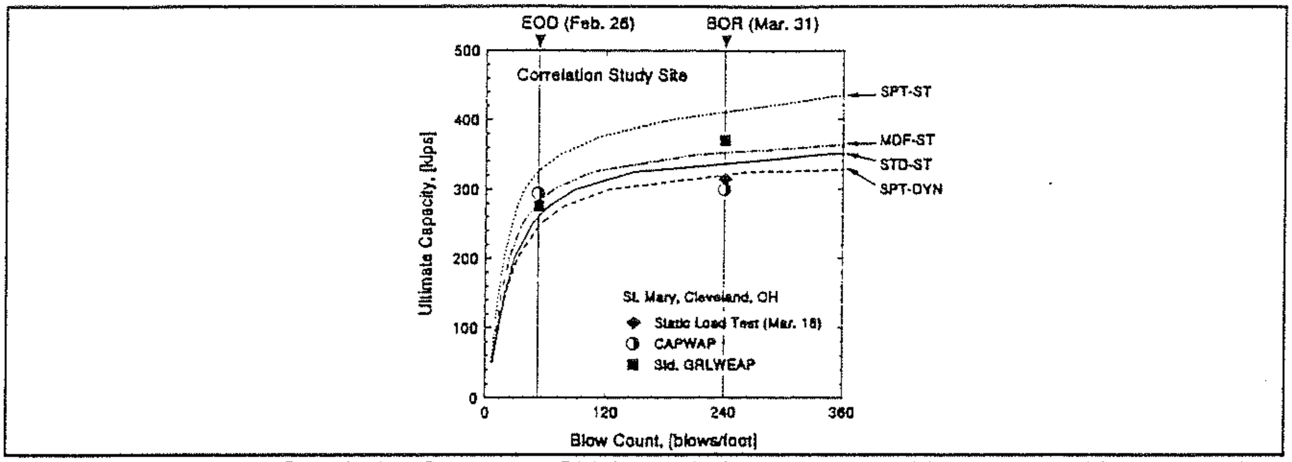

Figure 20: Bearing Graph for St. Mary, OH from Various Analysis Methods (1 kip = 4.45 kN; 1 blow/ft = 3.3 blows/m)

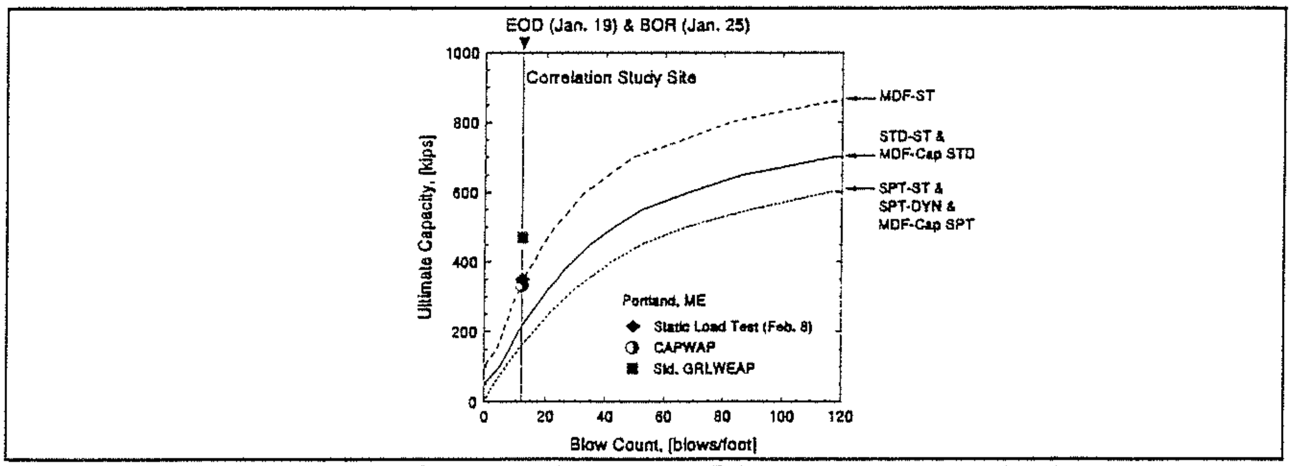

Figure 21: Bearing Graph for Portland, ME from Various Analysis Methods

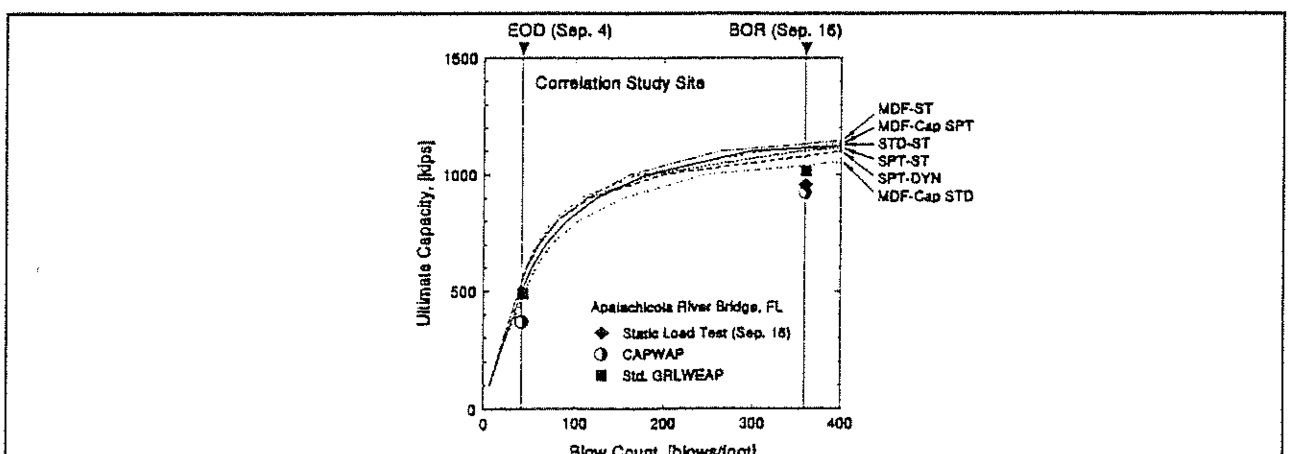

Figure 22: Bearing Graph for Apalachicola Bridge, FL from Various Analysis Methods

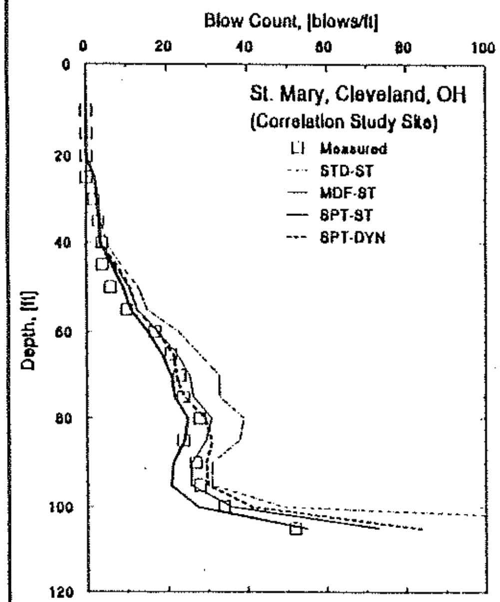

Figure 23: Drivability Graph for St. Mary, OH from Various Analysis Methods (1 ft = 0.305 m; 1 blow/ft = 3.3 blows/m)

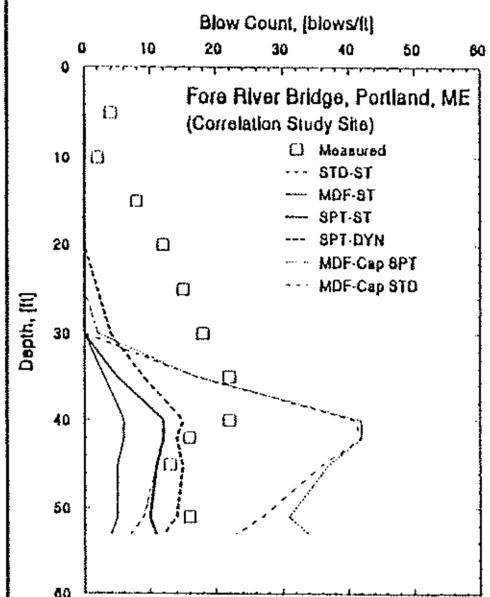

Figure 24: Drivability Graph for Portland, ME from Various Analysis Methods

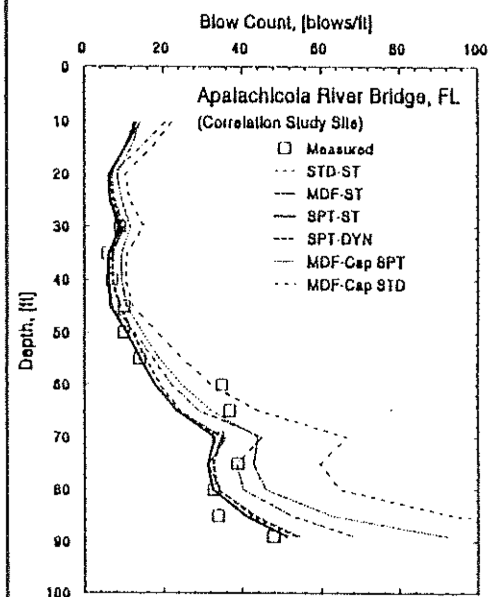

Figure 25: Drivability Graph for Apalachicola Bridge, FL from Various Analysis Methods

compared to the sampler end bearing. It was also found that the dynamic measurements generally yielded reliable toe or shaft resistance values compared to the static shaft or special tip measurements.

Shaft resistance values were usually low and did not allow for rate effect measurements that could be clearly distinguished from setup or other effects. However, where dynamic or static rate effects could be measured, calculation of the apparent exponent yielded unity which suggests that the original Smith damping approach was satisfactory. It is felt that the exponential damping law of the literature has only very limited practical applications.

Static unit toe resistance, both from sampler bottom and a special tip, showed good correlation with full scale test piles. For the shaft, for which both uplift and torque tests were performed, correction factors between 1.0 and 1.9 had to be applied to the sampler shaft unit resistance to yield agreement with full scale pile unit shaft resistance. Reasons for this correction might be a disturbed soil near the upper part of the sampler and a lower densification around the sampler compared to a large displacement pile. Granular soils required larger corrections than fine grained soils.

Static values calculated from "dynamic" analysis on the Modified SPT records showed good agreement with static values obtained from static uplift or compression tests performed with the Modified SPT, and with full scale test pile results.

The Modified SPT indicated relatively low toe damping factors in clay, *e.g.*, J_t = 0.03 s/ft (.1 s/m), for what was considered a driving situation (in contrast to restriking). Such low factors indeed yielded realistic blow counts for the full scale piles analyzed. Furthermore, low toe damping factors when applied to bearing capacity calculations would yield higher and therefore, on average, better EOD bearing capacity predictions. For granular soils, no clear tendency for the damping was observed.

Large quake sites can be identified from either "static" or "dynamic" analyses of data collected during the Modified SPT procedure. For the two sites, White City and Portland, that had indicated large full scale pile toe quakes, the Modified SPT also indicated relatively high quakes.

The Modified SPT results indicated that currently suggested shaft soil parameters are satisfactory for end of driving situations. These values are Smith shaft damping factors of 0.2 s/ft (0.66 s/m) for cohesive soils and 0.05 s/ft (0.16 s/m) for non-cohesive soils, and shaft quakes of 0.1 inch (2.5 mm). Admittedly, however, since sampler friction was always relatively low, the data had insufficient resolution for an accurate assessment of these values.

For restrike situations, a much greater variation in both shaft and toe damping must be expected. For example, tests in soft clays indicated very high restrike damping factors.

As for the Modified SPT procedure itself, it was, of course, more time consuming than normal SPT operations. However, since torque measurements can replace the uplift test and since dynamic measurements can replace the special tip static compression test, a significant improvement in the economy of the Modified SPT is possible.

REFERENCES

Beim, J. W., Paraiso, S. C., and Beim, G. K., 1992, "Dynamic Testing of enlarged base Franki Piles," Proceeding of the Fourth International Conference on the Application of Stress-Wave Theory to Piles, The Hague, The Netherlands, September, pp. 227-229.

Coyle H. M. and Gibson, G. C., 1970, "Empirical Damping Constants for Sands and Clays," Journal of the Soil Mechanics and Foundations Division, ASCE, Vol. 96, May.

Erickson, H., 1990, "Static Behavior of Driven Piles Estimated from Stress Wave Measurements on Dynamic Probes," Presented at the 1990 PDA Users Day, Gothenberg, Sweden.

Fellenius, B. H., Edde, R. D., and Beriault, L. L., 1992, "Dynamic and Static Testing for Pile Capacity in a Fine-Grained Soil," Proceeding of the Fourth International Conference on the Application of Stress-Wave Theory to Piles, The Hague, The Netherlands, September, pp. 401-408.

Goble, G. G. and Abou-matar, H., 1992, "Determination of Wave Equation Soil Constant from the Standard Penetration Test," Proceeding of the Fourth International Conference on the Application of Stress-Wave Theory to Piles, The Hague, The Netherlands, September, pp. 99-103.

Heerema, E. P. and De Jong A., 1979, "An Advanced Wave Equation Computer Program which Simulates Dynamic Pile Plugging through a Coupled Mass-Spring System," Proceeding International Conference on Numerical Methods in Offshore Piling, ICE, London, pp. 37-42.

Heerema, E. P., 1981, "Dynamic Point Resistance in Sand and in Clay, for Pile Driveability Analysis," Ground Engineering, Vol. 14, No. 6, pp.30-46.

Hussein, M. and Rausche, F., 1990, "Pile Design and Construction Control by Dynamic Method - a Case History," Geotechnical News, Vol. 8, No. 4, December.

Litkouhi, S. and Poskitt, T. J., 1980, "Damping Constant for Pile Driveability Calculations," Geotechnique, Vol. 30, No. 1, pp. 77-86.

Niyama, S., 1992, "Study on Open Toe Pile Driving Instrumentation Considering Soil Plug Effect in Sand," Proceeding of the Fourth International Conference on the Application of Stress-Wave Theory to Piles, The Hague, The Netherlands, September, pp. 299-304.

Randolph, M. F., 1977, "Modelling of the Soil Plug Response in Pile Driving," Proceeding 8th S. E. Asian Geotechnical Conference, Bangkok, 2:61-6.14.

Rausche, F., 1994, "Dynamic Pile Testing Around the World," Presented at the 1994 PDA Users Day, Orlando, FL, USA.

Rausche, F., Thendean, G., Abou-matar, H., Likins, G., and Goble, G., 1994, "Determination of Pile Driveability and Capacity from Penetration Tests," Draft Final Report Submitted to FHWA, Contract No. DTFH61-91-C-00047, October.

Schmertmann, J. H. and Palacios, A., 1979, "Energy Dynamics of SPT," Journal of the Geotechnical Engineering Division, ASCE, Vol. 105, No. GT8.

Seed, H. B., Tokimatsu, K., Harder, L. F., and Chung R. M., 1985, "Influence of SPT Procedures in Soil Liquefaction Resistance Evaluations," Journal of Geotechnical Engineering, ASCE, Vol. 111, No. 12, pp.1425-1448.

Skov, R. and Denver, H., 1988, "Time-dependence of Bearing Capacity of Piles," Proceedings of the Third International Conference on Application of Stress-Wave Theory on Piles, B. Fellenius editor, Ottawa, Canada, pp. 879-888.

Smith, E. A. L., 1960, "Pile Driving Analysis by the Wave Equation," Journal of the Soil Mechanics and Foundations Division, ASCE, Vol. 86, August.

1995
PDA USERS DAY

CLEVELAND, OH
(Sept. 15, 1995)